When be Temperate: On the Fitness Benefits of Lysis vs. Lysogeny

Guanlin Li[a], **Michael H.Cortez**[c], **and Joshua S. Weitz**[b,a]

[a]School of Physics, Georgia Institute of Technology, Atlanta, GA 30332; [b]School of Biological Sciences, Georgia Institute of Technology, Atlanta, GA 30332; [c]Department of Biological Science, Florida State University, Tallahassee, FL 32306

This manuscript was compiled on July 31, 2019

Bacterial viruses, i.e., 'bacteriophage', can infect and lyse their bacterial hosts, releasing new viral progeny. Yet temperate bacteriophage can also initiate lysogeny, i.e., a latent mode of infection, in which the viral genome is integrated into and replicated with the bacterial chromosome. Subsequently, the integrated viral genome, i.e., the 'prophage', can induce and restart the lytic pathway. The deferral of lysis has led to a long-standing question: why be temperate? Here, we explore the dependency of viral fitness on infection mode and ecological context. First, we use network loop analysis to show how a cell-centric metric of fitness (the basic reproduction number) decomposes into contributions to viral fitness from all possible infectious transmissions paths that start and end with infected cells. This analysis suggests that lysogeny should be favored at low host abundances and that induction should occur rarely when integration is favored – a finding that applies to a spectrum of mechanistic models of phage-bacteria dynamics spanning both explicit and implicit representations of intracellular infection dynamics. Second, we use invasion analyses to show when phage-bacteria communities with purely lytic and purely lysogenic endemic infections can and cannot be invaded by the other strategy. Our analysis reveals that lytic phage can, counter-intuitively, facilitate the subsequent invasion of latent strategies. Altogether, our results provide a framework for understanding the costs and benefits of being temperate.

Viral dynamics | Epidemiology | Latency | Eco-evolutionary dynamics | Microbial ecology

Viruses of microbes are ubiquitous in natural systems, e.g., densities of marine virus particles typically exceed 10^7 per ml and densities of viruses in the soil typically exceed 10^8 per ml. Viral infections can transform the fate of target cells, populations, and associated ecosystems (1, 2, 3, 4, 5). Bacteriophage infections can lead to lysis and death of the infected cell, and new infections by progeny virus particles can drive down microbial populations leading to endogenous oscillations in population densities (6, 7). However for many bacteriophage, lysis is not the only possible infection outcome.

Infection by temperate bacteriophage such as phage λ, μ, and P22 can lead to cell lysis or lysogeny (8, 9). The 'decision' process associated with lysis and lysogeny has been termed a genetic switch (10). In phage λ, the switch is modulated by a bidirectional promoter that controls expression of regulatory proteins whose stochastic expression and feedback culminates in either lysis or lysogeny (e.g., refer to (11) for a recent review). Notably, the probability of entering latency and the rate of spontaneous induction are both evolvable traits. The evolvability of quantitative traits associated with temperate phage raises the question: what are the direct benefits of lysogeny, i.e., why be temperate?

Prior hypotheses had suggested that temperate phage have an evolutionary advantage when few hosts are available and extracellular virion decay rates are high (12). In 1984, Frank Stewart and Bruce Levin addressed this question by analyzing nonlinear dynamics models of nutrients, cells, virulent phage and temperate phage (13). However, Stewart and Levin reported that "in spite of the intuitive appeal of this low density hypothesis, we are unable to obtain solutions consistent with it using the model presented here." Instead, they introduced external oscillations in resource supply rates in order to identify regimes in which both virulent and temperate bacteriophage could coexist. Moreover, by analyzing population abundances as a proxy for evolutionary success, the 'advantage' of a particularly lifestyle vs. another must be weighed in terms of relative abundances, e.g., comparing virus particles to infected cells. Such weightings are seemingly arbitrary and do not stem from an evolutionary framework.

Here, we re-asses the relationship between lytic versus lysogenic viral strategies and fitness by asking the question: under what conditions can temperate phage potentially outperform virulent phage? In other words, rather than asking why be temperate, we ask: when be temperate? To answer this question, we take two approaches. First, we adapt a cell-centric metric of viral invasion fitness - the basic reproductive number – $\mathcal{R}_0$ – to the ecological dynamics of viruses and their microbial hosts (14–16). Using Levins' network loop analysis (17), we show that seemingly intractable algebraic expressions for $\mathcal{R}_0$ can be biologically interpreted in terms of purely horizontal, vertical, and mixed transmission pathways. We use this decomposition of fitness to identify essential drivers of invasion for lysogenic and lytic strategies given fully susceptible populations. In doing so, we show that only purely lytic or purely latent strategies have the highest invasion fitness (*i.e.*, only purely lytic and purely latent strategies can maximize $\mathcal{R}_0$). We also show that our interpretation and results extend to the Stewart and Levin model and other recent mechanistic models of temperate phage ecology; see Fig. (1). Second, we use invasion analyses to identify when the endemic states of purely lytic and purely lysogenic strategies can and cannot be invaded by other viral strategies. As we show, the ecological conditions that favor lytic strategies can, counterintuitively, transform the community state to one that enables invasion by temperate phage. Overall, this analysis provides a theoretical framework for comparing latent and lytic viral strategies and deepens insights into the conditions under which latent viral strategies are favored in phage-bacteria communities.

No conflicts of interest.

[2]To whom correspondence should be addressed. E-mail: jsweitz@gatech.edu

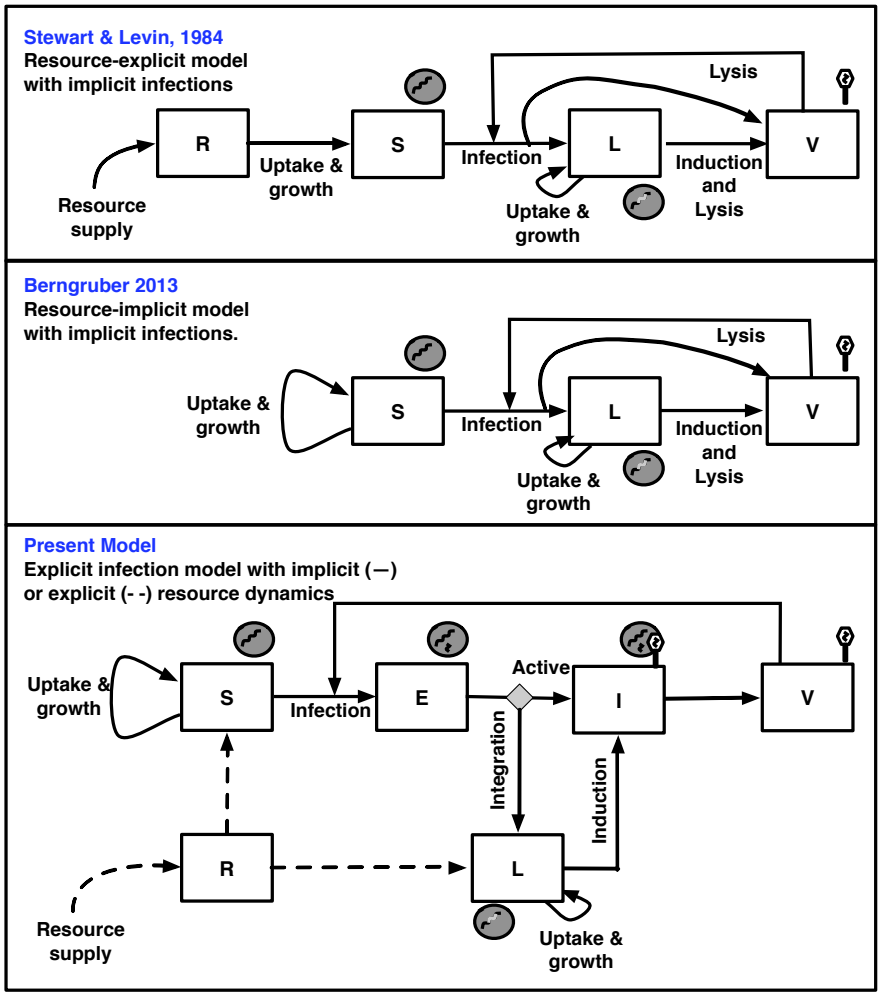

Fig. 1. Schematic of nonlinear dynamics population models of temperate phage. (Top) The resource-explicit model with implicit infections from Stewart and Levin, 1984 (13). (Middle) resource-implicit model with implicit infections from Berngruber et al, 2013 (15). (Bottom) The explicit infection model with implicit (–) or explicit (- -) resource dynamics (developed here). The nonlinear dynamics for each model are presented in *Methods* and *SI Text, section* 5.

Results

Viral invasion analysis. The spread of temperate viruses in a parasite-free environment can be analyzed in terms of the basic reproduction number $\mathcal{R}_0$, which denotes the average number of new infected cells produced by a single (typical) infected cell and its progeny virions in an otherwise susceptible population (14, 15, 16). The next-generation matrix (NGM) approach can be used to calculate $\mathcal{R}_0$ (18). Via NGM, the pathogen should spread when the largest eigenvalue of the NGM, is greater than one. This eigenvalue is equivalent to $\mathcal{R}_0$. We begin by considering the dynamics of temperate phage in a model that includes explicit representation of infections including cells that are either susceptible (S), exposed (E), actively infected (I), or lysogens (L), as well as virus particles (V), see the bottom panel of Fig. (1). In this model, the life history traits of a temperate phage are defined by two evolvable parameters: p, the probability a virus enters the lysogenic pathway and γ, the induction rate after a virus enters the lysogenic pathway.

For the model represented in Eq. [9], the NGM is denoted by Φ :

$$\Phi = \begin{bmatrix} \overbrace{(1-p)\mathcal{R}^{hor}}^{E\to I\to V\to E} + \overbrace{p\widetilde{\gamma}\mathcal{R}^{hor}}^{E\to L\to I\to V\to E} & \overbrace{\mathcal{R}^{hor}\left(\widetilde{\gamma}/\widetilde{\lambda}\right)}^{L\to I\to V\to E} \\ \overbrace{p\widetilde{\lambda}\mathcal{R}^{ver}(1-\widetilde{\gamma})}^{E\to L\to L} & \overbrace{\mathcal{R}^{ver}(1-\widetilde{\gamma})}^{L\to L} \end{bmatrix} \quad [1]$$

where $\widetilde{\gamma} = \gamma/(\gamma + d_L)$ is the probability induction occurs, $\widetilde{\lambda} = \lambda/(\lambda + d_E)$ is the probability exposed cells enter the lytic or lysogenic pathway, $\mathcal{R}^{hor}$ and $\mathcal{R}^{ver}$ are the basic reproduction numbers of purely lytic phage ($p = 0$) and purely lysogenic phage ($p = 1, \gamma = 0$), respectively :

$$\mathcal{R}^{hor} = \overbrace{\frac{\lambda}{\lambda + d_E}}^{E\to I}\overbrace{\left(\frac{\beta\ \eta}{\eta + d_I}\right)}^{I\to V}\overbrace{\left(\frac{\phi S^*}{\phi S^* + m}\right)}^{V\to E}$$
$$\mathcal{R}^{ver} = \overbrace{\frac{b_L}{d_L}}^{L\to L} . \quad [2]$$

where $S^* = K(1 - d_S/r_S)$ is the susceptible host density in the virus-free environment. The vertical contribution to fitness is modulated by infected cell growth rates, b_L, which in the resource-implicit and resource-explicit systems are $r_L\,(1 - S^*/K)$ and $\psi(R^*)$ respectively, where R^* is the resource concentration in the virus-free environment.

Notably, there are only two states (E and L) that can produce newly infected individuals, i.e., states E and L are *epidemiological birth states*. Each entry Φ_{ij} in the NGM represents the expected number of new infected individuals in state i (either L or E), generated by one infected individual at state j (either L or E), accounting for new infections that arise via the lytic and lysogenic pathways. For example, Φ_{11} accounts for the expected number of exposed cells E produced by a single exposed cell. The single exposed cell E has a probability $(1-p)\widetilde{\lambda}$ of entering the I state, of which a fraction $\eta/(\eta+d_I)$ of infected cells I will release viruses. Each infected cell produces β free virus particles given successful lysis. The factor $\phi S^*/(\phi S^*+m)$ denotes the probability that a free virus particle is adsorbed into a susceptible cell before it decays. As such, $(1-p)\mathcal{R}^{hor}$ is the expected number of newly infected exposed cells produced by a single exposed cell via a purely lytic pathway. Similarly, the single exposed cell E has a probability $p\widetilde{\lambda}$ of entering the L state and being induced from the lysogenic cell L to infected cell I with probability $\widetilde{\gamma}$. Thus, a single exposed cell produces $p\widetilde{\gamma}\mathcal{R}^{hor}$ newly infected exposed cells on average after a sequence of integration, induction, and lysis events. Altogether, the expected number of exposed cells produced by a single exposed cell is $\Phi_{11} = (1-p)\mathcal{R}^{hor}+p\widetilde{\gamma}\mathcal{R}^{hor}$. The other entries in the NGM can be interpreted similarly; the transmission pathways are labeled in Eq. [1] for each entry of the NGM.

In the event that phage cannot induce, i.e., $\gamma = 0$, then the basic reproduction number reduces to:

$$\mathcal{R}_0 = \max(\mathcal{R}^{ver}, (1-p)\mathcal{R}^{hor}), \qquad [3]$$

which corresponds to the viral invasion fitness associated with either lysis or lysogeny, but not both, as derived in (16). The use of a cell-centric metric enables direct comparisons of lytic and lysogenic pathways, i.e., even in the absence of particle production from lysogens. In the general case where induction is possible, i.e., $\gamma > 0$, then, the basic reproduction number $\mathcal{R}_0$ becomes:

$$\mathcal{R}_0 = \frac{1}{2}\left(\mathrm{Tr}(\Phi) + \sqrt{\mathrm{Det}(\Phi)^2 - 4\,\mathrm{Det}(\Phi)}\right), \qquad [4]$$

where the trace $\mathrm{Tr}(\Phi)$ is:

$$\mathrm{Tr}(\Phi) = \mathcal{R}^{hor}\widetilde{\gamma}p + (1-p)\mathcal{R}^{hor} + (1-\widetilde{\gamma})\mathcal{R}^{ver}, \qquad [5]$$

and the determinant $\mathrm{Det}(\Phi)$ is:

$$\mathrm{Det}(\Phi) = \mathcal{R}^{hor}\mathcal{R}^{ver}(1-p)(1-\widetilde{\gamma}). \qquad [6]$$

Notably, this formula for the basic reproduction number applies to all model variants of temperate phage dynamics listed in Fig. (1), see *SI Text, section* 2B. However, Eq. [4] poses multiple challenges for interpreting $\mathcal{R}_0$ not only for phage, but for generalized cases of host-pathogen dynamics with multiple transmission modes (19). It is the interpretation problem that we address next.

Interpreting $\mathcal{R}_0$ using Levins' loop analysis. Here, we use Levins' loop analysis (17) to interpret the basic reproduction number $\mathcal{R}_0$ arising in each of the models depicted in Fig. (1). Levins' loop analysis was developed for the analysis of feedbacks in ecological networks (17) - which we adapt to the study of the network of paths in the life history of an infectious pathogen. Loop analysis has been used previously to interpret $\mathcal{R}_0$ for discrete-time stage structured population dynamics (20). In another instance, previous work (21) focused on applications of loop analysis to models where the NGM only has a single non-zero eigenvalue whereas the NGM given by Eq. [1] has multiple non-zero eigenvalues. In the present context, we define a one-generation loop as the collection of paths that start in one infection class and ends in the same class without revisiting any classes. Next, we define a joint two-generation loop as a pair of one-generation loops that start and end in the same class. Finally, we define a disjoint two-generation loop as a pair of one-generation loops whose pathways do not share an epidemiological birth state.

Using these definitions, we denote the reproduction number of the lytic loop (1) as P_1, the reproduction number of the lysogenic loop (2) as P_2 and the reproduction number of the lyso-lytic loop (3) as P_3. The reproduction numbers of one-generation loops can be directly read-off from the NGM Φ, Eq. [1],

$$\begin{aligned}
&(1)\quad \text{Lytic loop}: \overbrace{(1-p)\mathcal{R}^{hor}}^{E\to I\to V\to E} = P_1\\
&(2)\quad \text{Lysogenic loop}: \overbrace{(1-\widetilde{\gamma})\mathcal{R}^{ver}}^{L\to L} = P_2\\
&(3)\quad \text{Lyso-lytic loop}: \overbrace{p\widetilde{\gamma}\mathcal{R}^{hor}}^{E\to L\to I\to V\to E} = P_3.
\end{aligned} \qquad [7]$$

Among all the pairs of one-generation loops, there are seven joint two-generation loops with permutations, e.g. (1)⊕(1), (2)⊕(2), (3)⊕(3), (1)⊕(3), (3)⊕(1), (2)⊕(3) and (3)⊕(2), and two disjoint pairs of loops, e.g. (1)⊕(2) and (2)⊕(1). Using the above, Eq. [4] for $\mathcal{R}_0$ can be rewritten in the following form:

$$\boxed{\begin{aligned}\mathcal{R}_0 = &\frac{1}{2}\left(P_1 + P_2 + P_3\right)\\ &+ \frac{1}{2}\left(\sqrt{P_1^2 + P_2^2 + P_3^2 + 2P_1P_3 + 2P_2P_3 - 2P_1P_2}\right).\end{aligned}} \qquad [8]$$

Notice that $P_1 + P_2 + P_3$ represents the sum of the one-generation loops and the terms in the square root represent the sum of the joint two-generation loops discounted by the disjoint loops. The contributions from all two-generation loops are discounted by the 1/2 exponent because the basic reproductive number focuses on reproductive output after one generation. Fig. (2) shows the equivalency between Eq. [8] and the loop-based interpretation.

Notably, the calculations of $\mathcal{R}_0$ for all temperate phage models in Fig. (1) can be expressed in the form of Eq. [8]. Table (1) summarizes the equivalencies of the component calculations for $\mathcal{R}_0$ in each of the models given a lytic loop, lysogenic loop, and a mixed loop. Moreover, this loop interpretation also applies to reduced versions of these models as long as

Table 1. Loop-based $\mathcal{R}_0$ Calculations for Temperate Phage Models

Temperate phage dynamics	Lytic loop P_1	Lysogenic loop P_2	Lyso-lytic loop P_3
Resource-explicit model with implicit infections (Stewart & Levin, 1984)	$\overbrace{(1-p)\left(\frac{\beta\phi S^*}{\rho}\right)}^{V\to V}$	$\overbrace{\frac{\psi(R^*)}{\gamma+\rho+\nu}}^{L\to L}$	$\overbrace{\left(\frac{\gamma}{\gamma+\rho+\nu}\right)}^{L\to V}\overbrace{\left(\frac{\beta\phi S^*}{\rho}\right)}^{V\to L}p$
Resource-implicit model with implicit infections (Berngruber, 2013)	$\overbrace{(1-p)\left(\frac{b\beta\phi S^*}{\phi S^*+m}\right)}^{V\to V}$	$\overbrace{\frac{r_L\delta\,(1-S^*/K)}{m+\gamma}}^{L\to L}$	$\overbrace{\left(\frac{\gamma}{\gamma+m}\right)}^{L\to V}\overbrace{\left(\frac{b\beta\phi S^*}{\phi S^*+m}\right)}^{V\to L}p$
Resource-explicit model with explicit infections (Present)	$\overbrace{(1-p)\left(\frac{\lambda}{\lambda+d_E}\right)}^{E\to I}\overbrace{\left(\frac{\beta\,\eta}{\eta+d_I}\right)}^{I\to V}\overbrace{\left(\frac{\phi S^*}{\phi S^*+m}\right)}^{V\to E}$	$\overbrace{\frac{r_L(1-S^*/K)}{\gamma+d_L}}^{L\to L}$	$\overbrace{p\left(\frac{\lambda}{\lambda+d_E}\right)}^{E\to L}\overbrace{\left(\frac{\gamma}{\gamma+d_L}\right)}^{L\to I}\overbrace{\left(\frac{\beta\,\eta}{\eta+d_I}\right)}^{I\to V}\overbrace{\left(\frac{\phi S^*}{\phi S^*+m}\right)}^{V\to E}$
Resource-implicit model with explicit infections (Present)	$\overbrace{(1-p)\left(\frac{\lambda}{\lambda+d_E}\right)}^{E\to I}\overbrace{\left(\frac{\beta\,\eta}{\eta+d_I}\right)}^{I\to V}\overbrace{\left(\frac{\phi S^*}{\phi S^*+m}\right)}^{V\to E}$	$\overbrace{\frac{\psi(R^*)}{\gamma+d_L}}^{L\to L}$	$\overbrace{p\left(\frac{\lambda}{\lambda+d_E}\right)}^{E\to L}\overbrace{\left(\frac{\gamma}{\gamma+d_L}\right)}^{L\to I}\overbrace{\left(\frac{\beta\,\eta}{\eta+d_I}\right)}^{I\to V}\overbrace{\left(\frac{\phi S^*}{\phi S^*+m}\right)}^{V\to E}$

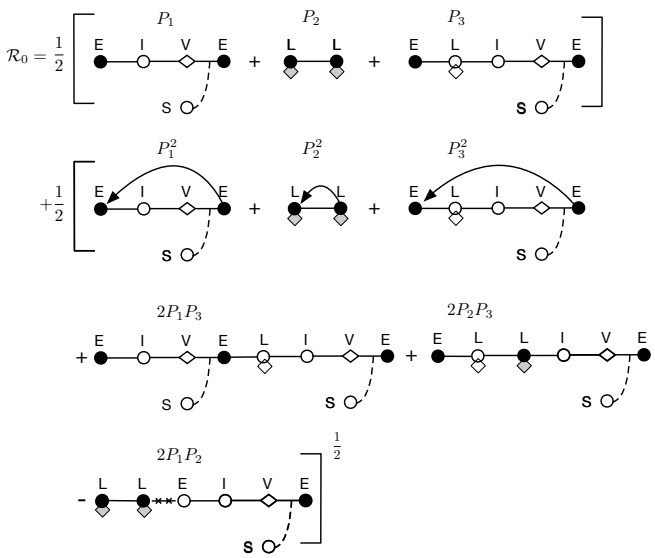

Fig. 2. Loop-based interpretation of the basic reproduction number for horizontal and vertical transmission of temperate phage. Closed circles denote epidemiological births, open circles represent infected cell transitions, diamonds represent virus particles, and lysogens are denoted using a hybrid symbol (denoting the presence of an integrated viral genome). Solid lines denote transitions between states, lines with arrows denote a repeat of the same loop, dashed lines denote interactions with uninfected cells, and lines with x-x denote non-feasible transitions.

they retain two epidemiological birth states (e.g., the $SILV$-system, as analyzed in (16)). Although the models differ in their mechanistic details, each shares two evolvable decision components: p, the probability of entering lysogenic state after infection and γ, the rate of induction from a lysogenic state. This similarity in form suggests that the dependence of invasion fitness (measured using $\mathcal{R}_0$) on the decision parameters p and γ may also transcend model details.

Maximal invasion fitness strategy. We systematically analyze the dependency of the viral invasion fitness $\mathcal{R}_0$ on the viral strategy (p, γ) for all four temperate phage models depicted in Fig. (1). Our goal is to identify which viral strategy maximizes the per-generation spread in a completely susceptible host population (*i.e.*, which strategy maximizes $\mathcal{R}_0$). In the two-dimensional viral strategy space we denote the purely lytic strategy as $p = 0$, and the purely lysogenic strategy as $p = 1, \gamma = \gamma_{min}$. As shown in the *SI Text, section* 3B, we find that the purely lytic strategy maximizes $\mathcal{R}_0$ when $\mathcal{R}^{hor} > \mathcal{R}^{ver}$, *i.e.*, more newly infected cells are produced through the lytic pathway than the lysogenic pathway. In contrast, the purely lysogenic strategy maximizes $\mathcal{R}_0$ when $\mathcal{R}^{hor} < \mathcal{R}^{ver}$, *i.e.*, more newly infected cells are produced through the lysogenic pathway than the lytic pathway. Notably, $\mathcal{R}^{ver}$ depends on susceptible host density S^* and resources R^* given resource-explicit dynamics while $\mathcal{R}^{hor}$ depends on the susceptible host density S^*.

Whether the purely lytic or purely lysogenic strategy maximizes $\mathcal{R}_0$ depends on the densities of susceptible hosts and resources in the virus-free environment. (We recognize that state-dependent viral life history traits also would influence this relationship; we return to this issue in the *Discussion*.) For the resource-implicit models, the virus-free environment is represented by the susceptible host density (S^*) while $\mathcal{R}^{ver}$ and $\mathcal{R}^{hor}$ are decreasing and increasing functions of susceptible host density, respectively. As a consequence, the strategy associated with maximal fitness ($\mathcal{R}_0$) switches from purely lysogenic at low densities, $S^* < S_c$ to purely lytic at high densities, $S^* > S_c$, see Fig. (3A) and Fig. (3B). The critical susceptible hosts density S_c satisfies $\mathcal{R}^{hor}(S_c) = \mathcal{R}^{ver}(S_c)$. This finding generalizes recent work contrasting viral invasion fitness for virulent, temperate, and chronic phage (16).

For the resource-explicit models, the virus-free environment is represented by the susceptible host density (S^*) and resource density (R^*). In the S^*-R^* plane, there is a critical transition curve (S_c, R_c) defined by $\mathcal{R}^{hor}(S_c) = \mathcal{R}^{ver}(R_c)$ where the strategy associated with maximal fitness (i.e., that maximizes $\mathcal{R}_0$) switches from purely lysogenic to purely lytic. This analysis reveals that a purely lysogenic strategy is favored given low cell abundances and high resources (above the (S_c, R_c) curve) and a purely lysogenic strategy is favored given high cell

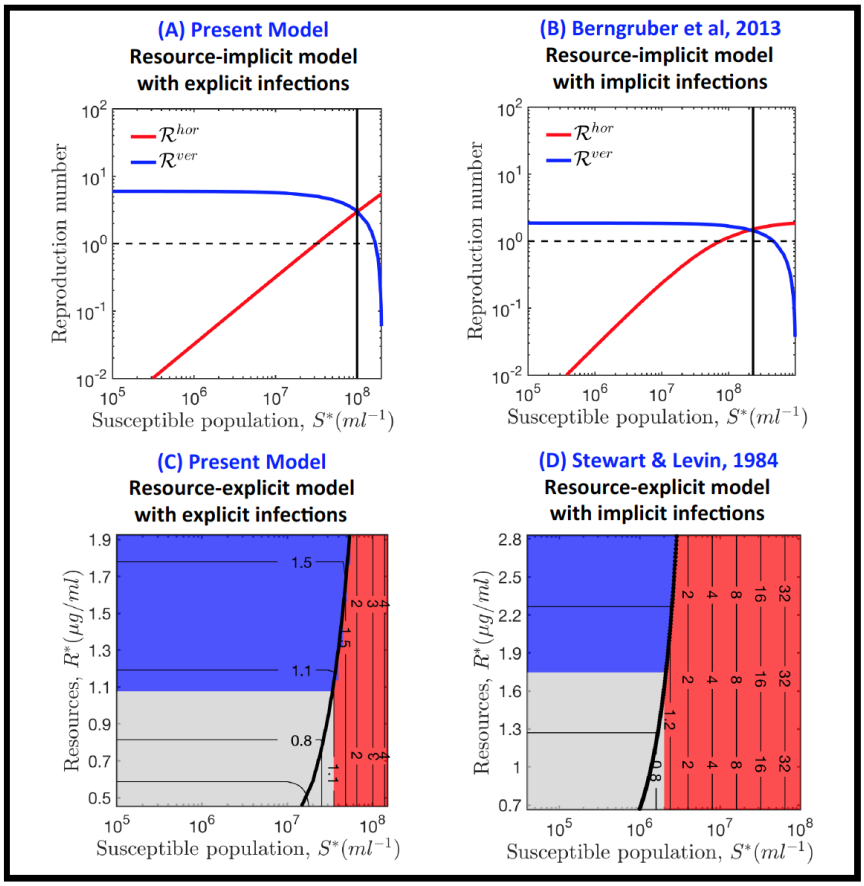

Fig. 3. The viral strategy that maximizes $\mathcal{R}_0$ in four temperate phage models depends on resource and host density in the virus-free environment. In the resource-implicit models, e.g. the present model with implicit resource dynamics (panel A) and Berngruber model (panel B), the purely lysogenic strategy ($p = 1, \gamma = \gamma_{min}$) maximizes $\mathcal{R}_0$ when $\mathcal{R}^{ver} > \mathcal{R}^{hor}$ and purely lytic strategy ($p = 0$) maximizes $\mathcal{R}_0$ when $\mathcal{R}^{ver} < \mathcal{R}^{hor}$. In the resource-explicit models, e.g. the present model with explicit resource dynamics (panel C) and Stewart and Levin model (panel D), the purely lysogenic strategy maximizes $\mathcal{R}_0$ when $\mathcal{R}^{ver} > \mathcal{R}^{hor}$ (blue region) and purely lytic strategy maximizes $\mathcal{R}_0$ when $\mathcal{R}^{ver} < \mathcal{R}^{hor}$ (red region). The gray area in panels C and D represent the viral strategies that maximize $\mathcal{R}_0$ still cannot invade the virus-free environments. See model parameters in *SI Text, section* 5

abundances and low resources (below the (S_c, R_c) curve), see Fig. (3C) and Fig. (3D). The rationale is that horizontal viral fitness is directly dependent on susceptible host cell density. In contrast, vertical viral fitness increases with increasing resource availability - which increases the replication rate of infected cells.

Notably, maximization of $\mathcal{R}_0$ does not necessarily predict long-term evolutionary dynamics (22, 23). One step towards characterizing evolutionary dynamics is to consider the initial, exponential growth rate of viruses which we denote σ. As shown in *SI Text, section* 2B, for the resource implicit model with explicit infections (Eqs. [9] and [10]), we compared the viral strategies that maximize σ and $\mathcal{R}_0$. We find that the purely lytic strategy maximizes both σ and $\mathcal{R}_0$ when the the susceptible hosts density is sufficiently high and the purely lysogenic strategy maximizes both σ and $\mathcal{R}_0$ when the susceptible hosts density is sufficiently low. The strategy that maximizes $\mathcal{R}_0$ switches at S_c but the strategy that maximizes σ switches at $S_c' \neq S_c$. Hence, a pure strategy – whether lysis or lysogeny – always maximizes fitness measured at the individual level (via $\mathcal{R}_0$) or at the population level (via σ), but which strategy is maximal depends on the chosen metric. The disagreement between outcomes given different metrics points toward the need to consider feedback when moving from short- to long-term dynamics.

Endemically infected states and viral invasion. The analysis presented thus far shows that viral invasion fitness (measured in terms of $\mathcal{R}_0$) is maximized by either purely temperate or purely lytic viral strategies, depending on host and nutrient densities. We next examine whether these maximal strategies are robust to invasion by other strategies. Specifically, we are interested in whether the endemic state for the strain that maximizes $\mathcal{R}_0$ can be invaded by other viral strains. To do so, we apply an invasion analysis (24) to the resource explicit model with explicit infections. We assume the resident strain has the viral strategy (p_r, γ_r) that maximizes $\mathcal{R}_0$, i.e., either the purely lytic strategy ($p = 0$) or the purely lysogenic strategy ($p = 1, \gamma = \gamma_{min}$). We then determine how a strategy (p_m, γ_m) of a mutant type competes in the environment determined by the resident. We note that the resident endemic equilibrium is stable given the particular parameter set in *SI Text, section* 5.

To begin, consider the case when the purely lysogenic strategy maximizes $\mathcal{R}_0$. In that case, we find that the resident lysogenic strategy cannot be invaded by any other strategies (see Fig. (4A) - blue area ; mathematical derivation in *SI*

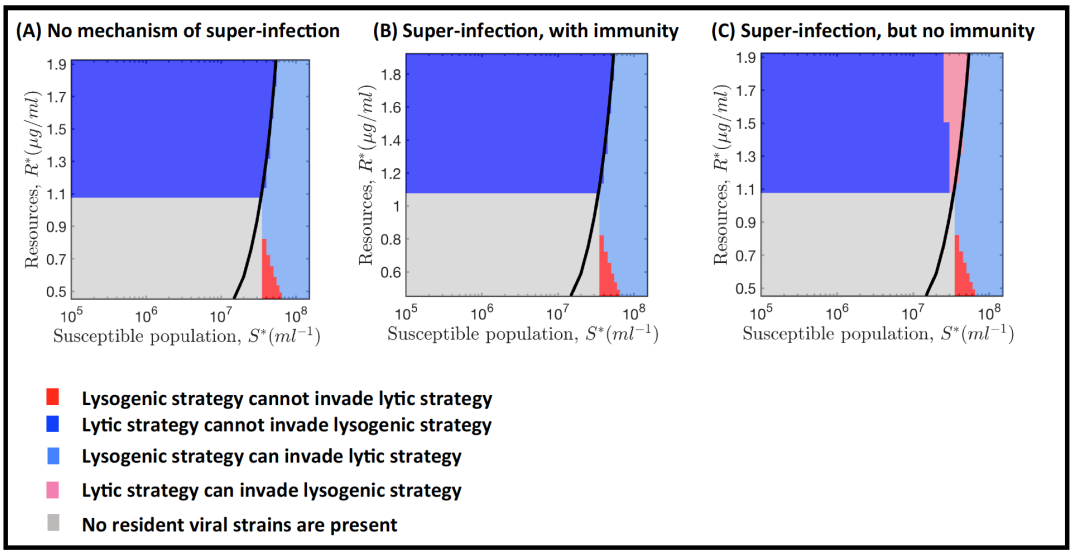

Fig. 4. Robustness of the viral strategies that maximize $\mathcal{R}_0$ for different super-infection scenarios. The resident strategy is a purely lysogenic strategy above the black curve and a purely lytic strategy below the black curve. Colors denote whether the other strategy can or cannot invade. See model parameters in *SI Text, section* 5.

Text, section 4B). The exclusion of lytic viruses by temperate viruses is a consequence of virus-host feedback. The temperate strategy is favored in the virus-free environment since the susceptible host density is low and the resource level is high. After viral invasion, the susceptible host density decreases and resources increase. In the event that lysogens confer a direct fitness benefit to cellular reproduction, then lysogens may outcompete susceptible cells. In either case, the resident endemic environment established by purely lysogenic strategy does not favor mutant viral strains with more lytic-like strategies (i.e., $0 \leq p_m < 1$ and $\gamma_m > \gamma_{min}$). Hence, the purely lysogenic strategy is evolutionarily robust.

Alternatively, consider the case when the purely lytic strategy maximizes $\mathcal{R}_0$. In this case, the resident lytic strategy can (but not always) be invaded by a temperate strategy (i.e., $0 < p_m \leq 1$), see *SI Text, section* 4B. Initially in the virus-free environment, the susceptible host density is high and resources are low. Lysis depletes susceptible hosts, which reduces niche competition between cells, thereby increasing the potential benefits of vertical transmission. This feedback implies that the vertical fitness can be higher than the horizontal fitness in the environment that lytic phage established, enabling more temperate strategies to invade (see Fig. (4A)) - light blue, purely lytic strategy can be invaded by more temperate strategies, and Fig. (4A) - red, purely lytic strategy is robust). This finding agrees with multiple recent studies of the evolution of viral strategies given long-term viral-host feedback (15, 25, 26). We also note that invasion by a mutant strain does not necessarily imply replacement of the resident strain.

We also explore the sensitivity of these findings to variations in the mechanistic details of super-infection. Super-infection denotes the possibility that a cell is infected by more than one virus (27). Super-infection becomes relevant from an ecological perspective when the resident virus reaches relatively high densities, *i.e.*, in the endemic context. Here, we consider two circumstances: (i) viruses are absorbed into all the cells but only actively infect susceptible cells (i.e., super-infection is a 'sink' for viruses); and (ii) purely lytic viruses are absorbed into all cells and can switch a lysogen into an actively infected cell (i.e., there is no super-infection 'immunity' (28)). Despite the differences in feedback mechanisms, we find that the regions of mutual invasion are roughly similar with one exception (contrast Fig. (4B/C) with Fig. (4A)). When there is no super-infection immunity, then the purely lysogenic strategy can be invaded by purely lytic strategy in some regions since lysogens become susceptible to lytic viruses (contrast Fig. (4B) and Fig. (4C)).

Discussion

We have demonstrated the benefits of the temperate phage lifestyle by exploring the dependency of viral invasion fitness on infection mode and ecological context. By integrating a cell-centric metric of viral invasion fitness (16) and Levins' loop analysis (17), we derive an interpretable representation of invasion fitness ($\mathcal{R}_0$) common to a series of mechanistic representations of temperate phage (see boxed Eq. [8] and Fig. (2)). In contrast to the previous application (21) of loop analysis, our work shows that the loop interpretation of $\mathcal{R}_0$ is useful even though the NGM has multiple non-zero eigenvalues. Using this form, we have shown that purely lyosgenic strategies maximize invasion fitness (i.e., $\mathcal{R}_0$) when resource density is relatively high and host density is relatively low (Fig. (3)). In addition, under these conditions, the endemic equilibrium of a virus with a purely temperate strategy cannot be invaded by more lytic strategies (Fig. (4)). In contrast, purely lytic strategies maximize invasion fitness when resource density is relatively low and host density is relatively high (Fig. (3)). However, even under these conditions, more temperate strategies can invade (bottom right Fig. (4A-C)). Altogether, our work identifies that may favor temperate strategies.

The benefits of being temperate can be decomposed into both short- and long-term components. In the short term, the invasion fitness $\mathcal{R}_0$ depends on the infection mode as well as an ecological context, e.g., susceptible cell density and resources. The invasion fitness reflects contributions from vertical, horizontal, and mixed transmission pathways. The

purely vertical fitness increases as resources increase or host abundances decrease, see Fig. (3). In contrast, the purely horizontal fitness increases as host abundances increase, see Fig. (3). As a consequence, we find that a purely lysogenic strategy maximizes $\mathcal{R}_0$ given low host abundances and high resources, whereas the purely lytic strategy maximizes $\mathcal{R}_0$ in environments with replete hosts. This relationship is consistent with observations that lysogeny is prevalence at times of low resources and low host availability, e.g., in aquatic systems (29, 30, 31). In practice, nutrient concentrations co-vary with host cell abundances, and so disentangling the effects of fluxes vs. pools will be critical to translating findings here to analysis of latency in the environment (32, 33, 34, 35, 36).

As a step toward understanding long-term evolution, we considered the invasibility of endemic states, and found that purely lysogenic strategies are not usually invasible by purely lytic strategies. This exclusion arises because lysogens diminish the susceptible host pool required for horizontal transmission and lytic viral invasion. In contrast purely lytic strategies are often invasible by temperate strategies. This susceptibility arises because lytic infections decrease susceptible host cell densities, and indirectly reduce niche competition between uninfected cells and a subpopulation of lysogens. Hence, our results provide direct support for the low host cell density adaptation hypothesis. We also evaluated the sensitivity of model findings to variation in superinfection exclusion. Despite the apparent robustness of temperate strategies to exclude purely lytic strategies, there is a notable exception: without superinfection exclusion, then lytic strategies can invade a community endemically infected by temperage phage. However, invasion need not imply replacement. Instead, invasion of an endemically infected state by temperate or purely lytic phage could lead to multi-strain coexistence – further complicating the benefits of being temperate.

While our study identifies possible conditions under which latency may evolve in phage-bacteria communities, additional theory is needed that explicitly models the long-term evolution of transmission strategies in viruses. For example, our analysis assumes that resources affect cell growth but not viral fitness. However, viral life history traits can, in fact, depend on resource levels and host physiological state (37, 38). Hence, future research should connect these microscopic traits with population level models. In addition, infected cell fate is strongly influenced by the cellular multiplicity of infection (cMOI), i.e., the number of co-infecting phage genomes in an individual cell. For phage λ, the fraction of lysogeny increases with increasing cMOI (39, 40, 41). The mechanistic basis for this change has focused on feedback in the cell fate determination circuit (42, 43, 44). However, the eco-evolutionary question of why such features have evolved remains an open question. Moving forward, the integration of resource dynamics, multiple infections, and fluctuating ecological dynamics (45) are critical to a comprehensive understanding of why phage are temperate. In doing so, it will also be important to recognize that what may be evolutionary 'optimal' in a single-host environment will likely differ in a complex community when multiple hosts and viruses interact (4). For example, a lysogen may not necessarily confer immunity to co-circulating viral types, providing potential advantages to lytic phage in complex communities relative to those in single host-virus populations.

In closing, the loop-based analysis developed here provides a unified and tractable interpretation of temperate phage invasion fitness. Lysogeny provides a direct fitness benefit to viruses when hosts are rare (but resources are available) and also enables viruses to invade environments in which lytic viruses have reduced host densities and by extension niche competition. We speculate that a loop-based approach to measuring invasion fitness may be of service in the analysis of other parasite-host systems. Altogether, our results provide a principled framework for connecting intracellular exploitation of bacteria by phage with population and evolutionary-level outcomes. We hope this framework can facilitate analysis of the experimental evolution of latency in model phage-bacteria systems as well as shed light on drivers of variation in lysogeny in the environment.

Methods

Main models. We represent the models in Fig. (1) in terms of systems of nonlinear ordinary differential equations (ODEs). First, the explicit infection model of temperate phage is

$$\begin{aligned}
\dot{S} &= \overbrace{b_S S}^{\text{growth}} - \overbrace{\phi S V}^{\text{infection}} - \overbrace{d_S S}^{\text{decay}} \\
\dot{E} &= \overbrace{\phi S V}^{\text{infection}} - \overbrace{\lambda E}^{\text{transition}} - \overbrace{d_E E}^{\text{decay}} \\
\dot{L} &= \overbrace{p\lambda E}^{\text{lysogenic infection}} + \overbrace{b_L L}^{\text{growth}} - \overbrace{\gamma L}^{\text{induction}} - \overbrace{d_L L}^{\text{decay}} \\
\dot{I} &= \overbrace{(1-p)\lambda E}^{\text{lytic infection}} + \overbrace{\gamma L}^{\text{induction}} - \overbrace{\eta I}^{\text{lysis}} - \overbrace{d_I I}^{\text{decay}} \\
\dot{V} &= \overbrace{\beta \eta I}^{\text{burst}} - \overbrace{\phi S V}^{\text{infection}} - \overbrace{m V}^{\text{decay}}
\end{aligned} \qquad [9]$$

where S, E, L, I and V denote the densities of susceptible cells, exposed infected cells, lysogens, lytic-fated infected cells, and virus particles respectively. Parameter ϕ is the adsorption rate, d_S, d_E, d_L and d_I are the cellular death rates of susceptible cells, exposed infected cells, lysogens and lytic-fated infected cells respectively, λ is the transition rate from exposed cells to the fate determined cells, p is the probability of lysogenization, γ is the induction rate, η is the lysis rate, β is the burst size and m is the virion decay rate. The growth rates of susceptible hosts and lysogens are denoted by b_S and b_L, respectively. For the resource-implicit model, the growth rates are

$$b_S(N) = r_S\left(1 - \frac{N}{K}\right), \quad b_L(N) = r_L\left(1 - \frac{N}{K}\right) \qquad [10]$$

where $N = S+E+L+I$ is the population density of total cells. Parameters r_S and r_L denote the maximal cellular growth rates of susceptible cells and lysogens, K is the carrying capacity. For the resource explicit model, the growth rates of susceptible hosts and lysogens are

$$b_S(R) = (1-\alpha_s)\psi(R), \quad b_L(R) = \psi(R) \qquad [11]$$

where R is the resource density and $\psi(R) = \mu_{max}R/(R_{in}+R)$ is the Monod equation. For the resource-explicit model, we add one additional equation to describe the dynamics of the resources,

$$\dot{R} = \overbrace{J}^{\text{influx}} - \overbrace{d_R R}^{\text{decay}} - \overbrace{f(R,S,L)}^{\text{uptake of nutrients}} \qquad [12]$$

where $f(R,S,L) = e\psi(R)\left(L + (1-\alpha_s)S\right)$ denotes the cumulative uptake of nutrients by all cells. Parameters μ_{max} and R_{in} are the maximal cellular growth rate and the half-saturation constant, J and d_R are the influx and decay rates of resources, e is the conversion efficiency, α_s is the selection coefficient that measures the relative difference in the reproductive output between lysogens and susceptible cells.

The resource-implicit model with implicit infections is

$$\begin{aligned}
\dot{S} &= \overbrace{r_S S\left(1-\frac{N}{K}\right)}^{\text{logistic growth}} + \overbrace{r_L(1-\delta)L\left(1-\frac{N}{K}\right)}^{\text{lysogens fail to transmit}} - \overbrace{b\phi SV}^{\text{infection}} - \overbrace{mS}^{\text{decay}} \\
\dot{L} &= \overbrace{r_L\delta L\left(1-\frac{N}{K}\right)}^{\text{logistic growth}} + \overbrace{pb\phi SV}^{\text{lysogenic path}} - \overbrace{\gamma L}^{\text{induction}} - \overbrace{mL}^{\text{decay}} \\
\dot{V} &= \overbrace{\beta\gamma L}^{\text{induction}} + \overbrace{(1-p)\beta b\phi SV}^{\text{lytic path}} - \overbrace{\phi NV}^{\text{absorption to cells}} - \overbrace{mV}^{\text{decay}}
\end{aligned} \tag{13}$$

where $N = S + L$ is the density of total cells, L is the density of infected cells, the susceptible cells density is S and the free-virus density is V. More details can be found in (15).

The resource-explicit model with implicit infections is

$$\begin{aligned}
\dot{R} &= \overbrace{\rho C}^{\text{media inflow}} - \overbrace{e\psi(R)\left(L + (1-\alpha_s)S\right)}^{\text{nutrient consumption}} - \overbrace{\rho R}^{\text{outflow}} \\
\dot{S} &= \overbrace{(1-\alpha_s)\psi(R)S}^{\text{growth with fitness selection}} - \overbrace{\phi SV}^{\text{infection}} + \overbrace{\nu L}^{\text{segregation}} - \overbrace{\rho S}^{\text{outflow}} \\
\dot{L} &= \overbrace{\psi(R)L}^{\text{growth}} + \overbrace{p\phi SV}^{\text{lysogenic infection}} - \overbrace{\gamma L}^{\text{induction}} - \overbrace{\nu L}^{\text{segregation}} - \overbrace{\rho L}^{\text{outflow}} \\
\dot{V} &= \overbrace{\beta\gamma L}^{\text{induction}} + \overbrace{\beta(1-p)\phi SV}^{\text{lytic infection}} - \overbrace{\phi LV}^{\text{absorption to lysogens}} - \overbrace{\rho V}^{\text{outflow}}
\end{aligned} \tag{14}$$

where R, S, L, and V denote the densities of resources, susceptible cells, lysogens and virus particles, respectively. This model describes the dynamics of microbial populations in the chemostat, ρ is the inflow (and outflow) rate; additional model details in (13).

Viral invasion analysis. The $\mathcal{R}_0$ calculations for each model variant closely follow the procedures given by Diekmann (18); complete calculations are provided in *SI Text, section* 2B. To demonstrate the biological interpretation of NGM associated with temperate phage invasion dynamics, we present the NGM, Φ, of model (9) in Eq. [1]. The loop-based $\mathcal{R}_0$ interpretation is inspired by Levins' loop analysis (17). For each model, we first compute $\mathcal{R}_0$ via Eq. [4] by an NGM approach, then, reformulate it into Eq. [8] by identifying all the one- and two-generation loops. The loop-based results are summarized in Table (1) and the detailed calculations are given in *SI Text, section* 2B-2C.

Endemic invasion analysis. For each temperate phage model, we construct the mutant–resident system, and compute the invasion fitness of mutant viral strains at the resident endemic equilibrium via a next-generation matrix approach (24, 25); see *SI Text, section* 4.

ACKNOWLEDGMENTS. We thank An Qi for reviewing code. This work was supported by a grant from the Simons Foundation (SCOPE Award ID 329108, J.S.W.).

1. Bergh Ø, BØrsheim KY, Bratbak G, Heldal M (1989) High abundance of viruses found in aquatic environments. *Nature* 340(6233):467.
2. Suttle CA (2005) Viruses in the sea. *Nature* 437(7057):356–361.
3. Breitbart M, Bonnain C, Malki K, Sawaya NA (2018) Phage puppet masters of the marine microbial realm. *Nature Microbiology* 3(7):754–766.
4. Weitz JS (2015) *Quantitative viral ecology: dynamics of viruses and their microbial hosts.* (Princeton University Press) Vol. 73.
5. Weinbauer MG (2004) Ecology of prokaryotic viruses. *FEMS Microbiology Reviews* 28(2):127–181.
6. Levin BR, Stewart FM, Chao L (1977) Resource-limited growth, competition, and predation: a model and experimental studies with bacteria and bacteriophage. *The American Naturalist* 111(977):3–24.
7. Lenski RE (1984) Coevolution of bacteria and phage: Are there endless cycles of bacterial defenses and phage counterdefenses? *Journal of Theoretical Biology* 108(3):319 – 325.
8. Lwoff A (1953) Lysogeny. *Bacteriological Reviews* 17(4):269–337. 13105613.
9. Bertani G (2004) Lysogeny at mid-twentieth century: P1, P2, and other experimental systems. *Journal of Bacteriology* 186(3):595–600.
10. Ptashne M (2004) *A genetic switch: phage lambda revisited.* (Cold Spring Harbor Laboratory Press Cold Spring Harbor, NY:) Vol. 3.
11. Golding I (2018) Infection by bacteriophage lambda: an evolving paradigm for cellular individuality. *Current Opinion in Microbiology* 43:9 – 13.
12. Levin BR, Lenski. RE (1983) Coevolution in bacteria and their viruses and plasmids. *Coevolution* pp. 99–127.
13. Stewart FM, Levin BR (1984) The population biology of bacterial viruses: Why be temperate. *Theoretical Population Biology* 26(1):93 – 117.
14. Gandon S (2016) Why be temperate: Lessons from bacteriophage . *Trends in Microbiology* 24(5):356 – 365.
15. Berngruber TW, Froissart R, Choisy M, Gandon S (2013) Evolution of virulence in emerging epidemics. *PLOS Pathogens* 9(3):1–8.
16. Weitz JS, Li G, Gulbudak H, Cortez MH, Whitaker RJ (2019) Viral invasion fitness across a continuum from lysis to latency. *Virus Evolution* 5(1):vez006.
17. Levins R (1974) Discussion paper: the qualitative analysis of partially specified systems. *Annals of the New York Academy of Sciences* 231(1):123–138.
18. Diekmann O, Heesterbeek JAP, Roberts MG (2010) The construction of next-generation matrices for compartmental epidemic models. *Journal of The Royal Society Interface* 7(47):873–885.
19. van den Driessche P (2017) Reproduction numbers of infectious disease models. *Infectious Disease Modelling* 2(3):288–303.
20. de Camino-Beck T, Lewis M (2007) A new method for calculating net reproductive rate from graph reduction with applications to the control of invasive species. *Bulletin of Mathematical Biology* 69(4):1341–1354.
21. Rueffler C, Metz JA (2013) Necessary and sufficient conditions for R_0 to be a sum of contributions of fertility loops. *Journal of Mathematical Biology* 66(4-5):1099–1122.
22. Cortez MH (2013) When does pathogen evolution maximize the basic reproductive number in well-mixed host–pathogen systems? *Journal of Mathematical Biology* 67(6):1533–1585.
23. Lion S, Metz JA (2018) Beyond R_0 maximisation: On pathogen evolution and environmental dimensions. *Trends in Ecology & Evolution* 33(6):458 – 473.
24. Hurford A, Cownden D, Day T (2010) Next-generation tools for evolutionary invasion analyses. *Journal of The Royal Society Interface* 7(45):561–571.
25. Wahl LM, Betti MI, Dick DW, Pattenden T, Puccini AJ (2019) Evolutionary stability of the lysis-lysogeny decision: Why be virulent? *Evolution* 73(1):92–98.
26. Gulbudak H, Weitz JS (2019) Heterogeneous viral strategies promote coexistence in virus-microbe systems. *Journal of Theoretical Biology* 462:65–84.
27. Abedon ST (2015) Bacteriophage secondary infection. *Virologica Sinica* 30(1):3–10.
28. van Houte S, Buckling A, Westra ER (2016) Evolutionary ecology of prokaryotic immune mechanisms. *Microbiology and Molecular Biology Reviews : MMBR* 80(3):745–763.
29. Payet JP, Suttle CA (2013) To kill or not to kill: The balance between lytic and lysogenic viral infection is driven by trophic status. *Limnology and Oceanography* 58(2):465–474.
30. Paul JH (2008) Prophages in marine bacteria: dangerous molecular time bombs or the key to survival in the seas? *The ISME journal* 2(6):579.
31. Warwick-Dugdale J, Buchholz HH, Allen MJ, Temperton B (2019) Host-hijacking and planktonic piracy: how phages command the microbial high seas. *Virology Journal* 16(1):15.
32. Weitz JS, Dushoff J (2008) Alternative stable states in host–phage dynamics. *Theoretical Ecology* 1(1):13–19.
33. Smith VH, Jones II TP, Smith MS (2005) Host nutrition and infectious disease: an ecological view. *Frontiers in Ecology and the Environment* 3(5):268–274.
34. Knowles B, et al. (2016) Lytic to temperate switching of viral communities. *Nature* 531(7595):466.
35. Weitz JS, Beckett SJ, Brum JR, Cael B, Dushoff J (2017) Lysis, lysogeny and virus–microbe ratios. *Nature* 549(7672):E1.
36. Knowles B, Rohwer F (2017) Knowles & rohwer reply. *Nature* 549(7672):E3.
37. Rabinovitch A, Hadas H, Einav M, Melamed Z, Zaritsky A (1999) Model for bacteriophage t4 development inescherichia coli. *Journal of Bacteriology* 181(5):1677–1683.
38. Clasen JL, Elser JJ (2007) The effect of host *Chlorella NC64A* carbon: phosphorus ratio on the production of *Paramecium bursaria Chlorella Virus-1*. *Freshwater Biology* 52(1):112–122.
39. Kourilsky P (1973) Lysogenization by bacteriophage lambda. *Molecular and General Genetics MGG* 122(2):183–195.
40. Kourilsky P (1975) Lysogenization by bacteriophage lambda: II.-identification of genes involved in the multiplicity dependent processes. *Biochimie* 56(11-12):1511–1516.
41. Kourilsky P, Knapp A (1975) Lysogenization by bacteriophage lambda: III.-multiplicity dependent phenomena occuring upon infection by lambda. *Biochimie* 56(11-12):1517–1523.
42. Weitz JS, Mileyko Y, Joh RI, Voit EO (2008) Collective decision making in bacterial viruses. *Biophysical Journal* 95(6):2673–2680.
43. Zeng L, et al. (2010) Decision making at a subcellular level determines the outcome of bacte-

riophage infection. *Cell* 141(4):682 – 691.
44. Golding I (2016) Single-cell studies of phage : Hidden treasures under occam's rug. *Annual Review of Virology* 3(1):453–472. PMID: 27482899.
45. Maslov S, Sneppen K (2015) Well-temperate phage: optimal bet-hedging against local environmental collapses. *Scientific Reports* 5:10523.

Supplementary Information for

When be Temperate: On the Fitness Benefits of Lysis vs. Lysogeny

Guanlin Li, Michael H.Cortez and Joshua S. Weitz

Joshua S. Weitz.
E-mail: jsweitz@gatech.edu

This PDF file includes:

Tables S1 to S4
References for SI reference citations

1. Main Models

A. The four model variants. The resource-implicit model with explicit infections from the main text is

$$
\begin{aligned}
\dot{S} &= \overbrace{r_S S\left(1-\frac{N}{K}\right)}^{\text{logistic growth}} - \overbrace{\phi S V}^{\text{infection}} - \overbrace{d_S S}^{\text{decay}} \\
\dot{E} &= \overbrace{\phi S V}^{\text{infection}} - \overbrace{\lambda E}^{\text{transition}} - \overbrace{d_E E}^{\text{decay}} \\
\dot{L} &= \overbrace{p\lambda E}^{\text{lysogenic infection}} + \overbrace{r_L L\left(1-\frac{N}{K}\right)}^{\text{logistic growth}} - \overbrace{\gamma L}^{\text{induction}} - \overbrace{d_L L}^{\text{decay}} \\
\dot{I} &= \overbrace{(1-p)\lambda E}^{\text{lytic infection}} + \overbrace{\gamma L}^{\text{induction}} - \overbrace{\eta I}^{\text{lysis}} - \overbrace{d_I I}^{\text{decay}} \\
\dot{V} &= \overbrace{\beta\eta I}^{\text{burst}} - \overbrace{\phi S V}^{\text{infection}} - \overbrace{m V}^{\text{decay}}
\end{aligned}
\qquad [1.1]
$$

where S, E, L, I and V denote the densities of susceptible cells, exposed infected cells, lysogens, lytic-fated infected cells and virus particles respectively, and $N = S + E + L + I$ is the total cell density. Parameters r_S and r_L denote the maximal cellular growth rates of susceptible cells and lysogens, K is the carrying capacity, ϕ is the adsorption rate, d_S, d_E, d_L and d_I are the cellular death rates of susceptible cells, exposed infected cells, lysogens and lytic-fated infected cells respectively, λ is the transition rate from exposed cells to the fate determined cells, p is the probability of lysogenization, γ is the induction rate, η is the lysis rate, β is the burst size and m is the virion decay rate.

The resource-implicit model with implicit infections in Berngruber et al. (2013) is

$$
\begin{aligned}
\dot{S} &= \overbrace{r_S S\left(1-\frac{N}{K}\right)}^{\text{logistic growth}} + \overbrace{r_L(1-\delta)L\left(1-\frac{N}{K}\right)}^{\text{lysogens fail to vertically transmit}} - \overbrace{b\phi S V}^{\text{infection}} - \overbrace{m S}^{\text{decay}} \\
\dot{L} &= \overbrace{r_L \delta L\left(1-\frac{N}{K}\right)}^{\text{logistic growth}} + \overbrace{p b\phi S V}^{\text{lysogenic path}} - \overbrace{\gamma L}^{\text{induction}} - \overbrace{m L}^{\text{decay}} \\
\dot{V} &= \overbrace{\beta\gamma L}^{\text{induction}} + \overbrace{(1-p)\beta b\phi S V}^{\text{lytic path}} - \overbrace{\phi N V}^{\text{absorption to cells}} - \overbrace{m V}^{\text{decay}}
\end{aligned}
\qquad [1.2]
$$

where $N = S + L$ is the density of total cells, L is the density of infected cells, the density of susceptible cells is S and the free-virus density is V. More details about model [1.2] can be found in (1).

The resource-explicit model with explicit infections from the main text is

$$
\begin{aligned}
\dot{R} &= \overbrace{J}^{\text{influx}} - \overbrace{e\psi(R)\left(L + (1-\alpha_s)S\right)}^{\text{cumulative uptake of nutrients by cells}} - \overbrace{d_R R}^{\text{decay}} \\
\dot{S} &= \overbrace{(1-\alpha_s)\psi(R)S}^{\text{growth with fitness selection}} - \overbrace{\phi S V}^{\text{infection}} - \overbrace{d_S S}^{\text{decay}} \\
\dot{E} &= \overbrace{\phi S V}^{\text{infection}} - \overbrace{\lambda E}^{\text{transition}} - \overbrace{d_E E}^{\text{decay}} \\
\dot{L} &= \overbrace{p\lambda E}^{\text{lysogenic infection}} + \overbrace{\psi(R)L}^{\text{lysogens growth}} - \overbrace{\gamma L}^{\text{induction}} - \overbrace{d_L L}^{\text{decay}} \\
\dot{I} &= \overbrace{(1-p)\lambda E}^{\text{lytic infection}} + \overbrace{\gamma L}^{\text{induction}} - \overbrace{\eta I}^{\text{lysis}} - \overbrace{d_I I}^{\text{decay}} \\
\dot{V} &= \overbrace{\beta\eta I}^{\text{burst}} - \overbrace{\phi S V}^{\text{infection}} - \overbrace{m V}^{\text{decay}}
\end{aligned}
\qquad [1.3]
$$

where R, S, E, L, I and V denote the densities of resources, susceptible cells, exposed infected cells, lysogens, lytic-fated infected cells and virus particles, respectively. The growth function $\psi(R) = \mu_{max}R/(R_{in} + R)$ is a Monod equation, where μ_{max} is the maximal cellular growth rate and R_{in} is the half-saturation constant. The parameters J and d_R are the influx and decay rates of resources, e is the host conversion efficiency, α_S is the selection coefficient that measures the relative fitness between lysogens and susceptible cells. All other parameters are defined as in model [1.1].

The resource-explicit model with implicit infections from Stewart and Levin (1984) is

$$
\begin{aligned}
\dot{R} &= \overbrace{\rho C}^{\text{media inflow}} - \overbrace{e\psi(R)\left(L + (1-\alpha_s)S\right)}^{\text{nutrient consumption}} - \overbrace{\rho R}^{\text{outflow}} \\
\dot{S} &= \overbrace{(1-\alpha_s)\psi(R)S}^{\text{growth with fitness selection}} - \overbrace{\phi S V}^{\text{infection}} + \overbrace{\nu L}^{\text{vegetative segregation from lysogens}} - \overbrace{\rho S}^{\text{outflow}} \\
\dot{L} &= \overbrace{\psi(R)L}^{\text{lysogens growth}} + \overbrace{p\phi S V}^{\text{lysogenic infection}} - \overbrace{\gamma L}^{\text{induction}} - \overbrace{\nu L}^{\text{vegetative segregation}} - \overbrace{\rho L}^{\text{outflow}} \\
\dot{V} &= \overbrace{\beta\gamma L}^{\text{induction}} + \overbrace{\beta(1-p)\phi S V}^{\text{lytic infection}} - \overbrace{\phi L V}^{\text{absorption to lysogens}} - \overbrace{\rho V}^{\text{outflow}}
\end{aligned}
\qquad [1.4]
$$

where R, S, L, and V denote the densities of resources, susceptible cells, lysogens and virus particles, respectively. Model [1.4] describes the dynamics of populations in a chemostat, where ρ is the inflow (and outflow) rate and ν is the segregation rate whereby lysogens become susceptible cells. See (2) for more details.

In the four model variants, the phage strategies are defined by two parameters: p defines the probability a virus enters the lysogenic pathway and γ defines the induction rate after a virus enters the lysogenic pathway. We define the viral strategy space Θ as

$$
\Theta \;=\; \{(p,\gamma) : 0 \le p \le 1,\ \gamma_{min} \le \gamma \le \gamma_{max}\} \qquad [1.5]
$$

where $\gamma_{min} > 0$.

B. From explicit infections to implicit infections. In this section, we show that the explicit infection models [1.1] and [1.3] can be reduced to the models with implicit infections via a quasi–steady–state (QSS) approximation.

For model [1.1] and model [1.3], we assume the (lysis-lysogeny decision) transition process and lysis process are extremely rapid in comparison to all the other biological processes. In other words, we let

$\lambda \gg d_E$ and $\eta \gg d_I$. The population dynamics of exposed cells from model [1.1] and model [1.3] can be rewritten as

$$\epsilon \dot{E} = \frac{\phi SV}{\lambda} - E(1 + \epsilon d_E) \approx \frac{\phi SV}{\lambda} - E \qquad [1.6]$$

where $\epsilon = 1/\lambda \ll 1$. Hence, the QSS equilibrium density of exposed cells population is $E^\epsilon = \phi SV/\lambda$. Using E^ϵ, the population dynamics of lytic-fated infected cells from model [1.1] and model [1.3] are rewritten as

$$\epsilon' \dot{I} = \frac{(1-p)\lambda E^\epsilon + \gamma L}{\eta} - I(1 + \epsilon' d_I) \approx \frac{(1-p)\phi SV + \gamma L}{\eta} - I \qquad [1.7]$$

where $\epsilon' = 1/\eta \ll 1$. Hence, the QSS equilibrium density of lytic-fated infected cells is $I^{\epsilon'} = [(1-p)\phi SV + \gamma L]/\eta$. Substituting E^ϵ and $I^{\epsilon'}$ into model [1.1] reduces it to the S, L, V-system with implicit infections,

$$\begin{aligned} \dot{S} &= r_S S\left(1 - \frac{N}{K}\right) - \phi SV - d_S S \\ \dot{L} &= p\phi SV + r_L L\left(1 - \frac{N}{K}\right) - \gamma L - d_L L \\ \dot{V} &= \beta(1-p)\phi SV + \beta\gamma L - \phi SV - mV. \end{aligned} \qquad [1.8]$$

Substituting E^ϵ and $I^{\epsilon'}$ into model [1.3] reduces it to the R, S, L, V-system with implicit infections,

$$\begin{aligned} \dot{R} &= J - e\psi(R)\left(L + (1-\alpha_s)S\right) - d_R R \\ \dot{S} &= (1-\alpha_s)\psi(R)S - \phi SV - d_S S \\ \dot{L} &= p\phi SV + \psi(R)L - \gamma L - d_L L \\ \dot{V} &= \beta(1-p)\phi SV + \beta\gamma L - \phi SV - mV. \end{aligned} \qquad [1.9]$$

2. $\mathcal{R}_0$-based Viral Invasion Analysis

A. Virus-free equilibrium. For the resource-implicit models [1.1] and [1.2], there are only susceptible cells (S^*) in the virus-free environments. The virus-free equilibrium of model [1.1] is

$$(S^*, 0, 0, 0, 0), \quad \text{where} \quad S^* = K\left(1 - \frac{d_S}{r_S}\right). \qquad [2.1]$$

The virus-free equilibrium of model [1.2] is

$$(S^*, 0, 0), \quad \text{where} \quad S^* = K\left(1 - \frac{d_S}{m}\right). \qquad [2.2]$$

For the resource-explicit models [1.3] and [1.4], there are both resources and susceptible cells (R^*, S^*) in the virus-free environments. The virus-free equilibrium of model [1.3] is

$$(R^*, S^*, 0, 0, 0, 0), \quad \text{where} \quad R^* = \frac{R_{in} d_S}{(1-\alpha_s)\mu_{max} - d_S} \quad \text{and} \quad S^* = \frac{J - d_R R^*}{e d_S}. \qquad [2.3]$$

The virus-free equilibrium of model [1.4] is

$$(R^*, S^*, 0, 0), \quad \text{where} \quad R^* = \frac{R_{in}\rho}{(1-\alpha_s)\mu_{max} - \rho} \quad \text{and} \quad S^* = \frac{C - R^*}{e}. \qquad [2.4]$$

B. Next-generation matrix approach. We start by computing the next-generation matrix (NGM) for the resource implicit model with explicit infections [1.1]. Consider the Jacobian of the model [1.1] evaluated at the virus-free equilibrium, Eq. [2.3]. We denote $\mathcal{J}$ as the submatrix of Jacobian for the E, L, I, V-subsystem. We decompose the submatrix as $\mathcal{J} = \mathcal{F} + \mathcal{V}$ where the transmission matrix $\mathcal{F}$ and the transition matrix $\mathcal{V}$ are

$$\mathcal{F} = \begin{bmatrix} 0 & 0 & 0 & \phi S^* \\ 0 & r_L(1-\frac{S^*}{K}) & 0 & 0 \\ 0 & 0 & 0 & 0 \\ 0 & 0 & 0 & 0 \end{bmatrix}, \quad \mathcal{V} = \begin{bmatrix} -(\lambda + d_E) & 0 & 0 & 0 \\ p\lambda & -(\gamma + d_L) & 0 & 0 \\ (1-p)\lambda & \gamma & -(\eta + d_I) & 0 \\ 0 & 0 & \beta\eta & -(\phi S^* + m) \end{bmatrix}.$$

Via NGM theory (3), the basic reproduction number $\mathcal{R}_0$ corresponds to the largest eigenvalue of the matrix $-\mathcal{F}\mathcal{V}^{-1}$, namely $\mathcal{R}_0 = \varrho(-\mathcal{F}\mathcal{V}^{-1})$ where $\varrho(M)$ is the spectral radius of the matrix M. There are two epidemiological birth states in model [1.1], hence, there are only two non-zero eigenvalues in $-\mathcal{F}\mathcal{V}^{-1}$. Here we introduce an augmented operator Q, where Q is a matrix in $\mathbb{R}^{4\times 2}$ with unit vectors in columns 1 and 2. The spectral radius of the 4×4 matrix $-\mathcal{F}\mathcal{V}^{-1}$ is the same as the spectral radius of the 2×2 matrix $-Q^T\mathcal{F}\mathcal{V}^{-1}Q$. For convenience, we define the next generation matrix of model [1.1] as

$$\Phi = -Q^T\mathcal{F}\mathcal{V}^{-1}Q = \begin{bmatrix} \Phi_{11} & \Phi_{12} \\ \Phi_{21} & \Phi_{22} \end{bmatrix},$$

where the entries of Φ are

$$\begin{aligned}
\Phi_{11} &= \overbrace{\left(\frac{p\lambda}{\lambda + d_E}\right)}^{E\to L}\overbrace{\left(\frac{\gamma}{\gamma + d_L}\right)}^{L\to I}\overbrace{\left(\frac{\beta\ \eta}{\eta + d_I}\right)}^{I\to V}\overbrace{\left(\frac{\phi S^*}{\phi S^* + m}\right)}^{V\to E} + \overbrace{\left(\frac{(1-p)\lambda}{\lambda + d_E}\right)}^{E\to I}\overbrace{\left(\frac{\beta\ \eta}{\eta + d_I}\right)}^{I\to V}\overbrace{\left(\frac{\phi S^*}{\phi S^* + m}\right)}^{V\to E} \\
\Phi_{22} &= \frac{\overbrace{r_L(1 - S^*/K)}^{L\to L}}{\gamma + d_L} \\
\Phi_{12} &= \overbrace{\left(\frac{\gamma}{\gamma + d_L}\right)}^{L\to I}\overbrace{\left(\frac{\beta\ \eta}{\eta + d_I}\right)}^{I\to V}\overbrace{\left(\frac{\phi S^*}{\phi S^* + m}\right)}^{V\to E} \\
\Phi_{21} &= \overbrace{\left(\frac{p\lambda}{\lambda + d_E}\right)}^{E\to L}\frac{\overbrace{r_L(1 - S^*/K)}^{L\to L}}{\gamma + d_L}.
\end{aligned} \tag{2.5}$$

Entry Φ_{ij} represents the expected number of new infected individuals in state i, generated by one infected individual at state j $(i, j = L, E)$, accounting for new infections that arise via the lytic and lysogenic pathways. Φ can be rewritten in terms of the basic reproductive number for viruses with purely lytic strategies ($p = 0$; $\mathcal{R}^{hor}$) and the basic reproductive number for viruses with purely lysogenic strategies ($p = 1, \gamma = 0$; $\mathcal{R}^{ver}$),

$$\Phi = \begin{bmatrix} \mathcal{R}^{hor}\widetilde{\gamma}p + (1-p)\mathcal{R}^{hor} & \mathcal{R}^{hor}(\widetilde{\gamma}/\widetilde{\lambda}) \\ \mathcal{R}^{ver}p\widetilde{\lambda}(1-\widetilde{\gamma}) & \mathcal{R}^{ver}(1-\widetilde{\gamma}) \end{bmatrix} \tag{2.6}$$

where

$$\widetilde{\gamma} = \frac{\gamma}{\gamma + d_L}, \quad \widetilde{\lambda} = \frac{\lambda}{\lambda + d_E}, \quad \mathcal{R}^{hor}(S^*) = \frac{\beta\eta\phi S^*\lambda}{(\eta + d_I)(\phi S^* + m)(\lambda + d_E)}, \quad \mathcal{R}^{ver}(S^*) = \frac{r_L}{d_L}\left(1 - \frac{S^*}{K}\right). \tag{2.7}$$

Next we compute the NGM for the implicit model with implicit infections [1.2]. We decompose the linearized infected subsystem of model [1.2], at the virus-free equilibrium, Eq. [2.2], into the transmission matrix $\mathcal{F}$ and the transition matrix $\mathcal{V}$:

$$\mathcal{F} = \begin{bmatrix} r_L\delta\left(1-\frac{S^*}{K}\right) & bp\phi S^* \\ 0 & (1-p)\beta b\phi S^* \end{bmatrix}, \quad \mathcal{V} = \begin{bmatrix} -(\gamma+m) & 0 \\ \gamma\beta & -(m+\phi S^*) \end{bmatrix}.$$

The NGM of model [1.2] is defined as

$$\Phi = -\mathcal{F}\mathcal{V}^{-1} = \begin{bmatrix} \overbrace{\frac{r_L\delta\left(1-\frac{S^*}{K}\right)}{\gamma+m}}^{L\to L} + \overbrace{\frac{\beta\gamma}{\gamma+m}}^{L\to V}\overbrace{\frac{pb\phi S^*}{(\phi S^*+m)}}^{V\to L} & \overbrace{pb\frac{\phi S^*}{\phi S^*+m}}^{V\to L} \\ \overbrace{\frac{\beta\gamma}{\gamma+m}}^{L\to V}\overbrace{(1-p)b\beta\frac{\phi S^*}{\phi S^*+m}}^{V\to V} & \overbrace{(1-p)b\beta\frac{\phi S^*}{\phi S^*+m}}^{V\to V} \end{bmatrix}. \tag{2.8}$$

As before, the NGM can be rewritten as

$$\Phi = \begin{bmatrix} \mathcal{R}^{hor}\widetilde{\gamma}p + (1-\widetilde{\gamma})\mathcal{R}^{ver} & \mathcal{R}^{hor}(p/\beta) \\ \mathcal{R}^{hor}(1-p)\widetilde{\gamma}\beta & \mathcal{R}^{hor}(1-p) \end{bmatrix} \tag{2.9}$$

where

$$\widetilde{\gamma} = \frac{\gamma}{\gamma+m}, \quad \mathcal{R}^{hor}(S^*) = \frac{b\beta\phi S^*}{\phi S^*+m}, \quad \mathcal{R}^{ver}(S^*) = \frac{r_L\delta}{m}\left(1-\frac{S^*}{K}\right). \tag{2.10}$$

Similarly, we compute the NGM for the resource explicit model with explicit infections [1.3]. We decompose the linearized infected subsystem of model [1.3] evaluated at the virus-free equilibrium, Eq. [2.3], into the transmission matrix $\mathcal{F}$ and transition matrix $\mathcal{V}$:

$$\mathcal{F} = \begin{bmatrix} 0 & 0 & 0 & \phi S^* \\ 0 & \psi(R^*) & 0 & 0 \\ 0 & 0 & 0 & 0 \\ 0 & 0 & 0 & 0 \end{bmatrix}, \quad \mathcal{V} = \begin{bmatrix} -(\lambda+d_E) & 0 & 0 & 0 \\ p\lambda & -(\gamma+d_L) & 0 & 0 \\ (1-p)\lambda & \gamma & -(\eta+d_I) & 0 \\ 0 & 0 & \beta\eta & -(\phi S^*+m) \end{bmatrix}.$$

The NGM of model [1.3] is defined as

$$\Phi = -Q^T\mathcal{F}\mathcal{V}^{-1}Q = \begin{bmatrix} \Phi_{11} & \Phi_{12} \\ \Phi_{21} & \Phi_{22} \end{bmatrix},$$

where Q is a matrix in $\mathbb{R}^{4\times 2}$ with unit vectors in columns 1 and 2. The entries of Φ are

$$\begin{aligned} \Phi_{11} &= \overbrace{\left(\frac{p\lambda}{\lambda+d_E}\right)}^{E\to L}\overbrace{\left(\frac{\gamma}{\gamma+d_L}\right)}^{L\to I}\overbrace{\left(\frac{\beta\ \eta}{\eta+d_I}\right)}^{I\to V}\overbrace{\left(\frac{\phi S^*}{\phi S^*+m}\right)}^{V\to E} + \overbrace{\left(\frac{(1-p)\lambda}{\lambda+d_E}\right)}^{E\to I}\overbrace{\left(\frac{\beta\ \eta}{\eta+d_I}\right)}^{I\to V}\overbrace{\left(\frac{\phi S^*}{\phi S^*+m}\right)}^{V\to E} \\ \Phi_{22} &= \overbrace{\frac{\psi(R^*)}{\gamma+d_L}}^{L\to L} \\ \Phi_{12} &= \overbrace{\left(\frac{\gamma}{\gamma+d_L}\right)}^{L\to I}\overbrace{\left(\frac{\beta\ \eta}{\eta+d_I}\right)}^{I\to V}\overbrace{\left(\frac{\phi S^*}{\phi S^*+m}\right)}^{V\to E} \\ \Phi_{21} &= \overbrace{\left(\frac{p\lambda}{\lambda+d_E}\right)}^{E\to L}\overbrace{\frac{\psi(R^*)}{\gamma+d_L}}^{L\to L}. \end{aligned} \tag{2.11}$$

As before, we can rewrite the NGM as

$$\Phi = \begin{bmatrix} \mathcal{R}^{hor}\tilde{\gamma}p + (1-p)\mathcal{R}^{hor} & \mathcal{R}^{hor}(\tilde{\gamma}/\tilde{\lambda}) \\ \mathcal{R}^{ver}p\tilde{\lambda}(1-\tilde{\gamma}) & \mathcal{R}^{ver}(1-\tilde{\gamma}) \end{bmatrix} \quad [2.12]$$

where

$$\tilde{\gamma} = \frac{\gamma}{\gamma + d_L}\ , \quad \tilde{\lambda} = \frac{\lambda}{\lambda + d_E}\ , \quad \mathcal{R}^{hor}(S^*) = \frac{\beta\eta\phi S^*\lambda}{(\eta + d_I)(\phi S^* + m)(\lambda + d_E)}\ , \quad \mathcal{R}^{ver}(R^*) = \frac{\psi(R^*)}{d_L}. \quad [2.13]$$

Finally, we compute the NGM for the resource explicit model with implicit infections [1.4]. We decompose the linearized infected subsystem of model [1.4], at the virus-free equilibrium, Eq. [2.4], in to the transmission matrix $\mathcal{F}$ and the transition matrix $\mathcal{V}$:

$$\mathcal{F} = \begin{bmatrix} \psi(R^*) & p\phi S^* \\ 0 & (1-p)\beta\phi S^* \end{bmatrix}\ , \quad \mathcal{V} = \begin{bmatrix} -(\rho+\gamma+\nu) & 0 \\ \gamma\beta & -\rho \end{bmatrix}.$$

The NGM of model [1.4] is defined as

$$\Phi = -\mathcal{F}\mathcal{V}^{-1} = \begin{bmatrix} \overbrace{\frac{\psi(R^*)}{\rho+\gamma+\nu}}^{L\to L} + \overbrace{\frac{\beta\gamma}{\rho+\gamma+\nu}}^{L\to V}\overbrace{p\frac{\phi S^*}{\rho}}^{V\to L} & \overbrace{p\frac{\phi S^*}{\rho}}^{V\to L} \\ \overbrace{\frac{\beta\gamma}{\rho+\gamma+\nu}}^{L\to V}\overbrace{(1-p)\frac{\beta\phi S^*}{\rho}}^{V\to V} & \overbrace{(1-p)\frac{\beta\phi S^*}{\rho}}^{V\to V} \end{bmatrix}. \quad [2.14]$$

As before, we can rewrite the NGM as

$$\Phi = \begin{bmatrix} \mathcal{R}^{hor}\tilde{\gamma}p + (1-\tilde{\gamma})\mathcal{R}^{ver} & \mathcal{R}^{hor}(p/\beta) \\ \mathcal{R}^{hor}(1-p)\tilde{\gamma}\beta & \mathcal{R}^{hor}(1-p) \end{bmatrix} \quad [2.15]$$

where

$$\tilde{\gamma} = \frac{\gamma}{\gamma+\rho+\nu}\ , \quad \mathcal{R}^{hor}(S^*) = \frac{\phi S^*\beta}{\rho}\ , \quad \mathcal{R}^{ver}(R^*) = \frac{\psi(R^*)}{\rho+\nu}. \quad [2.16]$$

Notably, the next-generation matrices for all four model variants are 2×2 matrices, as shown in Eq. [2.6], Eq. [2.8], Eq. [2.12] and Eq. [2.15]. The traces, $T(\Phi)$, and determinants, $D(\Phi)$, of each next-generation matrix can be written as

$$T(\Phi) = \mathcal{R}^{hor}\tilde{\gamma}p + (1-p)\mathcal{R}^{hor} + (1-\tilde{\gamma})\mathcal{R}^{ver}\ , \quad D(\Phi) = \mathcal{R}^{hor}\mathcal{R}^{ver}(1-p)(1-\tilde{\gamma}). \quad [2.17]$$

where the values of $\mathcal{R}^{hor}, \mathcal{R}^{ver}$ and $\tilde{\gamma}$ are given in Eq. [2.7], Eq. [2.10], Eq. [2.13] and Eq. [2.16]. The dominate eigenvalue $\mathcal{R}_0$ can be obtained from the trace and the determinant of the next-generation matrix,

$$\mathcal{R}_0 = \frac{1}{2}\left(T(\Phi) + \sqrt{T(\Phi)^2 - 4D(\Phi)}\right). \quad [2.18]$$

In general, $\mathcal{R}_0 = \max(\mathcal{R}^{hor}, (1-\tilde{\gamma})\mathcal{R}^{ver})$ when $p = 0$. However, we define $\mathcal{R}_0 = \mathcal{R}^{hor}$ when $p = 0$ because that matches the biological scenario defined by a virus with a purely lytic strategy.

C. Loop-based interpretation of $\mathcal{R}_0$. Motivated by Levins' loop analysis (4), we can rewrite Eq. [2.18] in a biological interpretable way. We define, $P_1 = (1-p)\mathcal{R}^{hor}$, $P_2 = (1-\tilde{\gamma})\mathcal{R}^{ver}$ and $P_3 = p\tilde{\gamma}\mathcal{R}^{hor}$. Then, Eq. [2.18] can be written as

$$2\mathcal{R}_0 = P_1 + P_2 + P_3 + \sqrt{P_1^2 + P_2^2 + P_3^2 + 2P_1P_3 + 2P_2P_3 - 2P_1P_2}. \quad [2.19]$$

A full description of this interpretation is presented in the main text.

3. Maximization of $\mathcal{R}_0$-based Viral Invasion Fitness

A. Preliminaries. A strategy (p^*, γ^*) maximizes the basic reproduction number corresponding to the viral invasion fitness as measured at the individual level if

$$\mathcal{R}_0(p^*, \gamma^*) \geq \mathcal{R}_0(p, \gamma) \quad \forall\ (p, \gamma) \in \Theta.$$

Given its use in the calculations and proofs, we note that while $\widetilde{\gamma} = \gamma/(\gamma + d_L)$ lies in the closed interval

$$\widetilde{\gamma} \in \left[\frac{\gamma_{min}}{\gamma_{min} + d_L}\ ,\ \frac{\gamma_{max}}{\gamma_{max} + d_L}\right] \quad \text{where} \quad 0 < \frac{\gamma_{min}}{\gamma_{min} + d_L} < \frac{\gamma_{max}}{\gamma_{max} + d_L} < 1,$$

we generally use $\widetilde{\gamma} \in (0, 1)$ instead of $\gamma \in [\gamma_{min}, \gamma_{max}]$ for convenience.

Proposition 3.1 *The basic reproduction number $\mathcal{R}_0(p, \gamma)$, Eq. [2.18], is marginal continuous on $(p, \gamma) \in \Theta$ and marginal differentiable on $(p, \gamma) \in \Theta$ except at $\left(0,\ \left(\frac{\mathcal{R}^{ver}}{\mathcal{R}^{hor}} - 1\right) d_L\right)$.*

Proof. The marginal continuity of $\mathcal{R}_0(p, \gamma)$ on $(p, \gamma) \in \Theta$ is obvious. Let $\theta \in \{p, \widetilde{\gamma}\}$, the derivative of $\mathcal{R}_0(p, \widetilde{\gamma})$ with respect to θ is

$$\frac{\partial \mathcal{R}_0}{\partial \theta} = \frac{1}{2}\left[T_\theta + \frac{T_\theta T - 2D_\theta}{\sqrt{T^2 - 4D}}\right]$$

where $T_\theta = \frac{\partial T}{\partial \theta}$ and $D_\theta = \frac{\partial D}{\partial \theta}$. Thus, we need $T^2 - 4D$ to be strictly positive to ensure the marginal differentiability. We write out $T^2 - 4D$ in terms of p and $\widetilde{\gamma}$

$$T^2 - 4D = \left[\mathcal{R}^{hor}(1-p) - \mathcal{R}^{ver}(1-\widetilde{\gamma})\right]^2 + 2\mathcal{R}^{hor}p\widetilde{\gamma}\left[\mathcal{R}^{hor}(1-p) + \mathcal{R}^{ver}(1-\widetilde{\gamma})\right] + (\mathcal{R}^{hor}p\widetilde{\gamma})^2\ .$$

Algebraic manipulation shows that $T^2 - 4D > 0$ everywhere in Θ except at $\left(0,\ \left(\frac{\mathcal{R}^{ver}}{\mathcal{R}^{hor}} - 1\right) d_L\right)$. □

Lemma 3.2 *Given a fixed γ satisfying $0 < \gamma_{min} \leq \gamma \leq \gamma_{max}$, the basic reproduction number $\mathcal{R}_0(p, \gamma)$ is uniquely maximized at $p^* = 1$ if $\mathcal{R}^{hor} < \mathcal{R}^{ver}$. In contrast, the basic reproduction number $\mathcal{R}_0(p, \gamma)$ is uniquely maximized at $p^* = 0$ if $\mathcal{R}^{hor} > \mathcal{R}^{ver}$.*

Proof. In the proof, we assume $\mathcal{R}^{hor} < \mathcal{R}^{ver}$; the case $\mathcal{R}^{hor} > \mathcal{R}^{ver}$ can be proved with a similar argument. The uniqueness of the maximal strategy p^* is showed by the strict monotonicity of $\mathcal{R}_0$ for all $p \in [0, 1]$. Calculating the derivative of $\mathcal{R}_0$ with respect to p yields

$$\begin{aligned}
\frac{\partial \mathcal{R}_0}{\partial p} > 0 \quad &\Leftrightarrow \quad \frac{1}{2}\left[T_p + \frac{T_p T - 2D_p}{\sqrt{T^2 - 4D}}\right] > 0 \\
&\Leftrightarrow \quad [4D_p - 2T_p T]^2 > 4T_p^2\left[T^2 - 4D\right] \\
&\Leftrightarrow \quad T_p^2 D > D_p T_p T - D_p^2
\end{aligned}$$

where the derivatives are $T_p = \mathcal{R}^{hor}(\widetilde{\gamma} - 1) < 0$ and $D_p = -\mathcal{R}^{hor}\mathcal{R}^{ver}(1 - \widetilde{\gamma}) < 0$. Note that

$$2T_p T - 4D_p = 2\mathcal{R}^{hor}(1-\widetilde{\gamma})\left[(\mathcal{R}^{ver} - \mathcal{R}^{hor}) + \mathcal{R}^{hor}p(1-\widetilde{\gamma}) + \widetilde{\gamma}(\mathcal{R}^{ver} - \mathcal{R}^{hor}p)\right] > 0\ .$$

Substitution yields

$$\begin{aligned}
&T_p^2 D > D_p T_p T - D_p^2 \\
&\quad \Leftrightarrow (\mathcal{R}^{hor})^2\mathcal{R}^{ver}(\widetilde{\gamma} - 1)^2\left[\mathcal{R}^{hor}\mathcal{R}^{ver}(1-\widetilde{\gamma})(1-p) - \mathcal{R}^{ver}(\mathcal{R}^{hor}\widetilde{\gamma}p + \mathcal{R}^{hor}(1-p) + \mathcal{R}^{ver}(1-\widetilde{\gamma}) - \mathcal{R}^{ver})\right] > 0 \\
&\quad \Leftrightarrow (\mathcal{R}^{hor})^2\mathcal{R}^{ver}(\widetilde{\gamma} - 1)^2\widetilde{\gamma}(\mathcal{R}^{ver} - \mathcal{R}^{hor}) > 0 \\
&\quad \Leftrightarrow \mathcal{R}^{ver} - \mathcal{R}^{hor} > 0\ .
\end{aligned}$$

Therefore, the basic reproduction number is a strictly monotone increasing function of p in the range of $[0, 1]$. This implies $\mathcal{R}_0$ is maximized at $p^* = 1$ and minimized at $p = 0$ by the continuity of $\mathcal{R}_0$. □

Lemma 3.3 *Given a fixed p satisfying $0 < p \leq 1$, the basic reproduction number $\mathcal{R}_0(p,\gamma)$ is uniquely maximized at $\gamma^* = \gamma_{min}$ if $\mathcal{R}^{hor} < \mathcal{R}^{ver}$. In contrast, the basic reproduction number $\mathcal{R}_0(p,\gamma)$ is uniquely maximized at $\gamma^* = \gamma_{max}$ if $\mathcal{R}^{hor} > \mathcal{R}^{ver}$.*

Proof. The proof is similar to the proof of lemma (3.2). According to proposition (3.1), we fix $p \neq 0$ such that $\mathcal{R}_0$ is differentiable on $\gamma_{min} \leq \gamma \leq \gamma_{max}$. We assume $\mathcal{R}^{hor} < \mathcal{R}^{ver}$; the proof for $\mathcal{R}^{hor} > \mathcal{R}^{ver}$ is similar. Note by the chain rule that

$$\frac{\partial \mathcal{R}_0}{\partial \gamma} = \frac{\partial \mathcal{R}_0}{\partial \widetilde{\gamma}} \frac{\partial \widetilde{\gamma}}{\partial \gamma} \quad \text{where} \quad \frac{\partial \widetilde{\gamma}}{\partial \gamma} > 0 \ .$$

Let $\widetilde{\gamma} \in (0,1)$. Differentiating $\mathcal{R}_0$ yields

$$\frac{\partial \mathcal{R}_0}{\partial \widetilde{\gamma}} \ = \ \frac{1}{2}\left[T_{\widetilde{\gamma}} + \frac{T_{\widetilde{\gamma}}T - 2D_{\widetilde{\gamma}}}{\sqrt{T^2 - 4D}}\right].$$

Given $\mathcal{R}^{hor} < \mathcal{R}^{ver}$, the derivatives are $T_{\widetilde{\gamma}} = \mathcal{R}^{hor}p - \mathcal{R}^{ver} < 0$ and $D_{\widetilde{\gamma}} = -\mathcal{R}^{hor}\mathcal{R}^{ver}(1-p) < 0$. The sign of $T_{\widetilde{\gamma}}T - 2D_{\widetilde{\gamma}}$ is unknown, which can be expanded as

$$T_{\widetilde{\gamma}}T - 2D_{\widetilde{\gamma}} = \widetilde{\gamma}(\mathcal{R}^{hor}p - \mathcal{R}^{ver})^2 + (\mathcal{R}^{hor})^2 p(1-p) + \mathcal{R}^{ver}(\mathcal{R}^{hor} - \mathcal{R}^{ver}) \quad .$$

If $T_{\widetilde{\gamma}}T - 2D_{\widetilde{\gamma}} \leq 0$ then $\frac{\partial \mathcal{R}_0}{\partial \widetilde{\gamma}} < 0$. If $T_{\widetilde{\gamma}}T - 2D_{\widetilde{\gamma}} > 0$, then

$$\begin{aligned}
\frac{\partial \mathcal{R}_0}{\partial \widetilde{\gamma}} < 0 \quad &\Leftrightarrow \quad \frac{1}{2}\left[T_{\widetilde{\gamma}} + \frac{T_{\widetilde{\gamma}}T - 2D_{\widetilde{\gamma}}}{\sqrt{T^2 - 4D}}\right] \ < \ 0 \\
&\Leftrightarrow \quad \left[4D_{\widetilde{\gamma}} - 2T_{\widetilde{\gamma}}T\right]^2 \ < \ 4T_{\widetilde{\gamma}}^2\left[T^2 - 4D\right] \\
&\Leftrightarrow \quad T_{\widetilde{\gamma}}^2 D \ < \ D_{\widetilde{\gamma}}T_{\widetilde{\gamma}}T - D_{\widetilde{\gamma}}^2 \\
&\Leftrightarrow \quad (\mathcal{R}^{hor})^2\mathcal{R}^{ver}(1-p)p(\mathcal{R}^{hor} - \mathcal{R}^{ver}) < 0 \\
&\Leftrightarrow \quad \mathcal{R}^{hor} < \mathcal{R}^{ver}.
\end{aligned}$$

Thus, if $\mathcal{R}^{hor} < \mathcal{R}^{ver}$ then $\frac{\partial \mathcal{R}_0}{\partial \widetilde{\gamma}} < 0$. This means the basic reproduction number is a strictly monotone decreasing function of γ when $\mathcal{R}^{hor} < \mathcal{R}^{ver}$. Thus, by the continuity of $\mathcal{R}_0$ is maximized at $\gamma^* = \gamma_{min}$ and minimized at $\gamma = \gamma_{max}$ uniquely. □

B. Maximization of $\mathcal{R}_0$. Using lemma (3.2) and lemma (3.3), we summarize the results of maximal viral strategy in the following theory.

Theorem 1 *The basic reproduction number $\mathcal{R}_0(p,\gamma)$, Eq. [2.18], is maximized at $p^* = 0$ and all $\gamma_{min} \leq \gamma \leq \gamma_{max}$ if $\mathcal{R}^{hor} > \mathcal{R}^{ver}$. On the other hand, $\mathcal{R}_0(p,\gamma)$ is maximized uniquely at $(p^*,\gamma^*) = (1,\gamma_{min})$ if $\mathcal{R}^{hor} < \mathcal{R}^{ver}$.*

Proof. The proof follows from lemma (3.2) and lemma (3.3). If $\mathcal{R}^{hor} > \mathcal{R}^{ver}$, then

$$\begin{aligned}
\max_{\gamma \in [\gamma_{min},\gamma_{max}]} \ \max_{p \in [0,1]} \mathcal{R}_0(p,\gamma) &= \max_{\gamma \in [\gamma_{min},\gamma_{max}]} \mathcal{R}_0(p^* = 0,\gamma) \\
&= \max_{\gamma \in [\gamma_{min},\gamma_{max}]} \ \max\{\mathcal{R}^{hor}, \ (1-\widetilde{\gamma})\mathcal{R}^{ver}\} \\
&= \mathcal{R}^{hor} \qquad \forall \ \gamma \in [\gamma_{min},\gamma_{max}].
\end{aligned}$$

On the other hand, if $\mathcal{R}^{hor} < \mathcal{R}^{ver}$, then

$$\begin{aligned}\max_{\gamma\in[\gamma_{min},\gamma_{max}]}\max_{p\in[0,1]}\mathcal{R}_0(p,\gamma) &= \max_{\gamma\in[\gamma_{min},\gamma_{max}]}\mathcal{R}_0(p^*=1,\gamma)\\ &= \max_{\gamma\in[\gamma_{min},\gamma_{max}]}\tilde{\gamma}\mathcal{R}^{hor}+(1-\tilde{\gamma})\mathcal{R}^{ver}\\ &= \mathcal{R}_0(1,\gamma_{min}).\end{aligned}$$

□

Remark 1 *We note the following:*
(i) $\mathcal{R}_0(p,\gamma)$ *is bounded above by* $max(\mathcal{R}^{hor},\mathcal{R}^{ver})$ *and bounded below by* $min(\mathcal{R}^{hor},\mathcal{R}^{ver})$.
(ii) If $\mathcal{R}^{hor}=\mathcal{R}^{ver}$, *then* $\mathcal{R}_0(p,\gamma)=\mathcal{R}^{hor}$ *for all* $(p,\gamma)\in\Theta$.
(iii) If $min(\mathcal{R}^{hor},\mathcal{R}^{ver})>1$, *then* $\mathcal{R}_0(p,\gamma)>1$ *for all* $(p,\gamma)\in\Theta$.
(iv) If $max(\mathcal{R}^{hor},\mathcal{R}^{ver})<1$, *then* $\mathcal{R}_0(p,\gamma)<1$ *for all* $(p,\gamma)\in\Theta$.

Remark 2 *For the two resource-implicit models [1.1] and [1.2], theorem (1) can be restated in terms of the density of susceptible hosts at the virus-free equilibrium* (S^*). *Specifically, because* $\mathcal{R}^{hor}$ *is a monotonically increasing function of* S^* *and* $\mathcal{R}^{ver}$ *is a monotonically decreasing function of* S^*, *there exists a critical value* S_c *that satisfies* $\mathcal{R}^{hor}(S_c)=\mathcal{R}^{ver}(S_c)$. *Thus, we can restate theorem (1) in terms of* S^*: *If* $S^*>S_c$, *then* $\mathcal{R}^{hor}>\mathcal{R}^{ver}$ *and the maximal strategy is* $p^*=0$ *and arbitrary* $\gamma\in[\gamma_{min},\gamma_{max}]$. *If* $S^*<S_c$, *then* $\mathcal{R}^{hor}<\mathcal{R}^{ver}$ *and the maximal strategy is* $p^*=1$ *and* $\gamma=\gamma_{min}$.

Remark 3 *For the two resource-explicit models [1.3] and [1.4], theorem (1) can be restated in terms of the resource concentration and the density of susceptible hosts at the virus-free equilibrium* (R^*,S^*). *Specifically, because* $\mathcal{R}^{hor}$ *is a monotonically increasing function of* S^* *and* $\mathcal{R}^{ver}$ *is a monotonically increasing function of* R^*, *there exists a curve in* R^*,S^**-space where there is a transition from the purely lytic strategy* ($p=0$) *maximizing* $\mathcal{R}_0$ *to the purely lysogenic strategy* ($p=1,\gamma=\gamma_{min}$) *maximizing* $\mathcal{R}_0$. *That curve is defined by* $\Gamma=\{(R^*,S^*):\mathcal{R}^{hor}(S^*)-\mathcal{R}^{ver}(R^*)=0\}$. *We decompose* R^*,S^**-space into two regions based on* Γ, *let* $\Gamma_+=\{(R^*,S^*):\mathcal{R}^{hor}(S^*)-\mathcal{R}^{ver}(R^*)>0\}$ *and* $\Gamma_-=\{(R^*,S^*):\mathcal{R}^{hor}(S^*)-\mathcal{R}^{ver}(R^*)<0\}$. *Thus, we can restate theorem (1) in terms of* R^* *and* S^*: *If* $(R^*,S^*)\in\Gamma_+$, *then* $\mathcal{R}^{hor}>\mathcal{R}^{ver}$ *and the maximal strategy is* $p^*=0$ *and arbitrary* $\gamma\in[\gamma_{min},\gamma_{max}]$. *If* $(R^*,S^*)\in\Gamma_-$, *then* $\mathcal{R}^{hor}<\mathcal{R}^{ver}$ *and the maximal strategy is* $p^*=1$ *and* $\gamma=\gamma_{min}$.

Remark 4 *Let* σ *denote the largest eigenvalue of the linearized infected subsystem,* $\mathcal{J}$. *Biologically,* σ *is the exponential growth rate of viral strategy in a virus-free host population. Both* σ *and* $\mathcal{R}_0$ *can be used to predict viral invasion because* $sign\{\sigma\}=sign\{\mathcal{R}_0-1\}$. *The values of* σ *and* $\mathcal{R}_0$ *may not be maximized at by the same viral strategy. We numerically explored what viral strategies maximized* σ *in model [1.1]. Our numerical results showed that there exists a critical density of susceptible hosts,* S_c', *such that if* $S^*>S_c'$ *then* σ *is maximized at* $p^*=0$ *and arbitrary* $\gamma\in(\gamma_{min},\gamma_{max})$ *and if* $S^*<S_c'$ *then* σ *is maximized at* $p^*=1$ *and* $\gamma=\gamma_{min}$. *However, the critical values* S_c *and* S_c' *are not the same; see Table (S1) for an example. Thus, in general, the viral strategy that maximizes* $\mathcal{R}_0$ *is not the strategy that maximizes instantaneous growth rate.*

4. Endemic Invasion Analysis

In this section, we provide details about the evolutionary analysis for the four model variants. In doing so, we apply an invasion analyses (5), in which the system reaches a stable endemic equilibrium with a resident viral strategy $(p_r,\gamma_r)\in\Theta$. Further, we assume the resident strain is either the purely lytic ($p=0$) or purely lysogenic strategy ($p=1,\gamma=\gamma_{min}$). We then introduce a mutant viral strain with strategy $(p_m,\gamma_m)\in\Theta$ and determine if the mutant can invade the resident equilibrium. We start by deriving the next-generation matrix of the mutant at the resident equilibrium.

A. Next-generation matrix approach of evolutionary invasion analysis. The mutant-resident system of model [1.1] is

$$\begin{aligned}
\dot{S} &= r_S S\left(1-\frac{N}{K}\right) - \phi SV - \phi SV_m - d_S S \\
\dot{E} &= \phi SV - (\lambda + d_E)E \\
\dot{L} &= p_r \lambda E + r_L L\left(1-\frac{N}{K}\right) - (\gamma_r + d_L)L \\
\dot{I} &= (1-p_r)\lambda E + \gamma_r L - (\eta + d_I)I \\
\dot{V} &= \beta\eta I - \phi SV - mV \\
\dot{E}_m &= \phi SV_m - (\lambda + d_E)E_m \\
\dot{L}_m &= p_m \lambda E_m + r_L L_m\left(1-\frac{N}{K}\right) - (\gamma_m + d_L)L_m \\
\dot{I}_m &= (1-p_m)\lambda E_m + \gamma_m L_m - (\eta + d_I)I_m \\
\dot{V}_m &= \beta\eta I_m - \phi SV_m - mV_m
\end{aligned} \qquad [4.1]$$

where $N = S + E + L + I + E_m + L_m + I_m$ is the total population of hosts. The E_m, L_m, I_m, V_m-subsystem denotes the classes with the mutant viral strategies. The resident endemic equilibrium of system [4.1] is $(S^+, E^+, L^+, I^+, V^+, 0, 0, 0, 0)$. Invasion of the resident endemic equilibrium is determined by the magnitude of the maximum eigenvalue of the next generation matrix,

$$\Phi_r^m = \begin{bmatrix} \mathcal{R}_+^{hor}\widetilde{\gamma_m}p_m + (1-p_m)\mathcal{R}_+^{hor} & \mathcal{R}_+^{hor}(\widetilde{\gamma}_m/\widetilde{\lambda}) \\ \mathcal{R}_+^{ver}p_m\widetilde{\lambda}(1-\widetilde{\gamma}_m) & \mathcal{R}_+^{ver}(1-\widetilde{\gamma}_m) \end{bmatrix} \qquad [4.2]$$

where

$$\widetilde{\gamma_m} = \frac{\gamma_m}{\gamma_m + d_L}, \quad \widetilde{\lambda} = \frac{\lambda}{\lambda + d_E}, \quad \mathcal{R}_+^{hor}(S^+) = \frac{\beta\eta\phi S^+\lambda}{(\eta + d_I)(\phi S^+ + m)(\lambda + d_E)}, \quad \mathcal{R}_+^{ver}(N^+) = \frac{r_L}{d_L}\left(1-\frac{N^+}{K}\right) \qquad [4.3]$$

and $N^+ = S^+ + E^+ + L^+ + I^+$. The largest eigenvalue of Φ_r^m is denoted by $\mathcal{R}_0(p_m, \gamma_m|p_r, \gamma_r)$. The sign of $\mathcal{R}_0(p_m, \gamma_m|p_r, \gamma_r) - 1$ determines the invasion of the resident endemic equilibrium in system [4.1].

Similarly, we add the L_m, V_m-subsystem to model [1.2]. The resident endemic equilibrium of the augmented resident-mutant system of model [1.2] is denoted by $(S^+, L^+, V^+, 0, 0)$. The next-generation matrix of a mutant strain with viral strategy (p_m, γ_m) is

$$\Phi_r^m = \begin{bmatrix} \mathcal{R}_+^{hor}\widetilde{\gamma_m}p_m + (1-\widetilde{\gamma_m})\mathcal{R}_+^{ver} & \mathcal{R}_+^{hor}(p_m/\beta) \\ \mathcal{R}_+^{hor}(1-p_m)\widetilde{\gamma_m}\beta & \mathcal{R}_+^{hor}(1-p_m) \end{bmatrix} \qquad [4.4]$$

where

$$\widetilde{\gamma_m} = \frac{\gamma_m}{\gamma_m + m}, \quad \mathcal{R}_+^{hor} = \frac{b\beta\phi S^+}{\phi N^+ + m}, \quad \mathcal{R}^{ver} = \frac{r_L\delta}{m}\left(1-\frac{N^+}{K}\right) \qquad [4.5]$$

and $N^+ = S^+ + L^+$.

Again, we add the E_m, L_m, I_m, V_m-subsystem to model [1.3]. The resident endemic equilibrium of the augmented resident-mutant system of model [1.3] is denoted by $(R^+, S^+, E^+, L^+, I^+, V^+, 0, 0, 0, 0)$. The next-generation matrix of a mutant strain with viral strategy (p_m, γ_m) is

$$\Phi_r^m = \begin{bmatrix} \mathcal{R}_+^{hor}\widetilde{\gamma_m}p_m + (1-p_m)\mathcal{R}_+^{hor} & \mathcal{R}_+^{hor}(\widetilde{\gamma_m}/\widetilde{\lambda}) \\ \mathcal{R}_+^{ver}p_m\widetilde{\lambda}(1-\widetilde{\gamma_m}) & \mathcal{R}_+^{ver}(1-\widetilde{\gamma_m}) \end{bmatrix} \qquad [4.6]$$

where

$$\widetilde{\gamma_m} = \frac{\gamma_m}{\gamma_m + d_L}\ , \quad \widetilde{\lambda} = \frac{\lambda}{\lambda + d_E}\ , \quad \mathcal{R}_+^{hor}(S^+) = \frac{\beta\eta\phi S^+\lambda}{(\eta + d_I)(\phi S^+ + m)(\lambda + d_E)}\ , \quad \mathcal{R}_+^{ver}(R^+) = \frac{\psi(R^+)}{d_L}. \tag{4.7}$$

Finally, we add the L_m, V_m-subsystem to model [1.4]. The resident endemic equilibrium of the augmented resident-mutant system of model [1.4] is denoted by $(R^+, S^+, L^+, V^+, 0, 0)$. The next-generation matrix of a mutant strain with viral strategy (p_m, γ_m) is

$$\Phi_r^m = \begin{bmatrix} \mathcal{R}_+^{hor}\widetilde{\gamma_m}p_m + (1-\widetilde{\gamma_m})\mathcal{R}_+^{ver} & \mathcal{R}_+^{hor}(p_m/\beta) \\ \mathcal{R}_+^{hor}(1-p_m)\widetilde{\gamma_m}\beta & \mathcal{R}_+^{hor}(1-p_m) \end{bmatrix} \tag{4.8}$$

where

$$\widetilde{\gamma_m} = \frac{\gamma_m}{\gamma_m + \rho + \nu}\ , \quad \mathcal{R}_+^{hor}(S^+) = \frac{\phi S^+\beta}{\rho}\ , \quad \mathcal{R}_+^{ver}(R^+) = \frac{\psi(R^+)}{\rho + \nu}. \tag{4.9}$$

Notably, the derived next-generation matrices for the mutant strains in all four model variants are 2×2 matrices. The traces, $T(\Phi_r^m)$, and determinants, $D(\Phi_r^m)$ of four next-generation matrices are written as

$$T(\Phi_r^m) = \mathcal{R}_+^{hor}\widetilde{\gamma_m}p_m + (1-p_m)\mathcal{R}_+^{hor} + (1-\widetilde{\gamma_m})\mathcal{R}_+^{ver}\ , \quad D(\Phi_r^m) = \mathcal{R}_+^{hor}\mathcal{R}_+^{ver}(1-p_m)(1-\widetilde{\gamma_m}), \tag{4.10}$$

where the $\mathcal{R}_+^{hor}, \mathcal{R}_+^{ver}$ and $\widetilde{\gamma_m}$ are given in Eq. [4.3], Eq. [4.5], Eq. [4.7] and Eq. [4.9]. The dominate eigenvalue $\mathcal{R}_0(p_m, \gamma_m|p_r, \gamma_r)$ can be obtained from the trace and the determinant of the next-generation matrix,

$$\mathcal{R}_0(p_m, \gamma_m|p_r, \gamma_r) = \frac{1}{2}\left(T(\Phi_r^m) + \sqrt{T(\Phi_r^m)^2 - 4D(\Phi_r^m)}\right). \tag{4.11}$$

Using the fact that $\mathcal{R}_0(p_m, \gamma_m|p_r, \gamma_r) = 1$ when $(p_m, \gamma_m) = (p_r, \gamma_r)$, and the monotonicity of $\mathcal{R}_0(p_m, \gamma_m|p_r, \gamma_r)$ on $(p_m, \gamma_m) \in \Theta$ provided by lemma (3.2), lemma (3.3) and theorem (1), we immediately obtain the following theorem.

Theorem 2 *For all of the four model variants, we assume the susceptible cell population is positive at the stable resident endemic equilibrium, i.e., $S^+ > 0$. Then, we have:*

(i) If $\mathcal{R}_+^{hor} < \mathcal{R}_+^{ver}$, viral strains with more lysogenic strategies (i.e., $p_r < p_m \leq 1$ and $\gamma_{min} \leq \gamma_m < \gamma_r$) can invade, and viral strains with more lytic strategies (i.e., $0 \leq p_m < p_r$ and $\gamma_r < \gamma_m \leq \gamma_{max}$) cannot invade.

(ii) If $\mathcal{R}_+^{hor} > \mathcal{R}_+^{ver}$, viral strains with more lysogenic strategies (i.e., $p_r < p_m \leq 1$ and $\gamma_{min} \leq \gamma_m < \gamma_r$) cannot invade, and viral strains with more lytic strategies (i.e., $0 \leq p_m < p_r$ and $\gamma_r < \gamma_m \leq \gamma_{max}$) can invade.

Remark 5 *For model [1.1] and model [1.3], the stable resident endemic equilibrium might be a boundary equilibrium with $S^+ = 0$. If the resident system reaches a stable endemic equilibrium with $S^+ = 0$, then no mutant strain can invade. Specifically, a mutant strain is introduced at the resident equilibrium through a virus particle, the first step in the proliferation of a virus is that it infects a susceptible cell, hence, a virus mutant cannot spread given the absence of a susceptible population.*

B. Applications in two model variants: robustness of maximal strategies. Theorem (2) requires the specification of the resident equilibrium to determine whether mutant invasion scenarios correspond to case (i) or case (ii). In this section, we provide additional results to apply theorem (2) to model [1.1] and model [1.3].

Proposition 4.1 *(i) The stable resident endemic equilibrium of model [1.1], $(S^+, E^+, L^+, I^+, V^+)$ with $S^+ > 0$, satisfies $S^+ < N^+ < S^*$, where S^* is given by Eq. [2.1].*

(ii) The stable resident endemic equilibrium of model [1.3], $(R^+, S^+, E^+, L^+, I^+, V^+)$ with $S^+ > 0$, satisfies $R^+ > R^*$ and $S^+ < S^*$, where R^* and S^* are given by Eq. [2.3].

Proof. Proof of (i) : $S^+ < N^+$ is a trivial observation. We prove $N^+ < S^*$ by contradiction. Suppose $N^+ \geq S^*$ and set $\dot{S} = 0$ in model [1.1]

$$0 = S^+ \left[r_S \left(1 - \frac{N^+}{K} \right) - d_S \right] - \phi S^+ V^+ \leq -\phi S^+ V^+ < 0 \ .$$

This shows a contradiction such that (i) is true.

Proof of (ii) : At the stable resident endemic equilibrium of model [1.3], we set $\dot{R} = 0$ and $\dot{S} = 0$

$$\begin{cases} 0 = & J - d_R R^+ - e\psi(R^+) \left(L^+ + (1-\alpha_s) S^+ \right) \\ 0 = & S^+ \left[(1-\alpha_s)\psi(R^+) - \phi V^+ - d_S \right] \end{cases}$$

Given $S^+ > 0$, we rewrite the above system and find that

$$S^+ = \frac{(J - d_R R^+) - e\psi(R^+) L^+}{e(d_S + \phi V^+)}, \quad \psi(R^+) = \frac{\phi V^+ + d_S}{1 - \alpha_s}$$

Note that $\psi(R^*) = d_S/(1-\alpha_s)$ by substituting virus-free equilibrium, Eq. [2.3], into the Monod equation. Then, we find that

$$\psi(R^+) = \frac{\phi V^+ + d_S}{1 - \alpha_s} > \frac{d_S}{1 - \alpha_s} = \psi(R^*).$$

It should be clear that $R^+ > R^*$ since ψ, the Monod equation, is a strictly monotone increasing function. In addition,

$$S^+ = \frac{(J - d_R R^+) - e\psi(R^+) L^+}{e(d_S + \phi V^+)} < \frac{(J - d_R R^*)}{e d_S} = S^*.$$

□

Proposition 4.2 *(i) If the virus-free equilibrium of model [1.1] satisfies $\mathcal{R}^{hor}(S^*) < \mathcal{R}^{ver}(S^*)$, where $\mathcal{R}^{hor}(S^*)$ and $\mathcal{R}^{ver}(S^*)$ are given by Eq. [2.7], then $\mathcal{R}^{hor}_+(S^+) < \mathcal{R}^{ver}_+(N^+)$ at the stable resident endemic equilibrium, where $\mathcal{R}^{hor}_+(S^+)$ and $\mathcal{R}^{ver}_+(N^+)$ are given by Eq. [4.3].*

(ii) If the virus-free equilibrium of model [1.3] satisfies $\mathcal{R}^{hor}(S^*) < \mathcal{R}^{ver}(R^*)$, where $\mathcal{R}^{hor}$ and $\mathcal{R}^{ver}$ are given by Eq. [2.13], then $\mathcal{R}^{hor}_+(S^+) < \mathcal{R}^{ver}_+(R^+)$ at the stable resident endemic equilibrium, where $\mathcal{R}^{hor}_+(S^+)$ and $\mathcal{R}^{ver}_+(R^+)$ are given by Eq. [4.7].

Proof. Proof of (i): First, we assume that the susceptible cells population at resident equilibrium of model [1.1] is positive, $S^+ > 0$, then we have $S^+ < N^+ < S^*$ by proposition (4.1). Given $\mathcal{R}^{hor}(S^*) < \mathcal{R}^{ver}(S^*)$ in Eq. [2.7], we arrive

$$\mathcal{R}^{ver}_+(N^+) > \mathcal{R}^{ver}(S^*) > \mathcal{R}^{hor}(S^*) > \mathcal{R}^{hor}_+(S^+).$$

Second, if $S^+ = 0$ at the resident equilibrium of model [1.1], $\mathcal{R}^{hor}_+ = 0$, it's clear that $\mathcal{R}^{ver}_+ > \mathcal{R}^{hor}_+$.

Proof of (ii): First, we assume that the susceptible cells population at resident equilibrium of model [1.3] is positive, $S^+ > 0$, then we have $S^+ < S^*$ and $R^+ > R^*$ by proposition (4.1). Given $\mathcal{R}^{hor}(S^*) < \mathcal{R}^{ver}(R^*)$ in Eq. [2.13], we arrive

$$\mathcal{R}^{ver}_+(R^+) > \mathcal{R}^{ver}(R^*) > \mathcal{R}^{hor}(S^*) > \mathcal{R}^{hor}_+(S^+).$$

Second, if $S^+ = 0$ at the resident equilibrium of model [1.3], $\mathcal{R}^{hor}_+ = 0$, it's clear that $\mathcal{R}^{ver}_+ > \mathcal{R}^{hor}_+$. □

For model [1.1] and model [1.3], when the resident strains are either the purely lytic strategy ($p = 0$) or the purely lysogenic strategy ($p = 1, \gamma = \gamma_{min}$), some qualitative results of evolutionary invasion are immediately obtained by theorem (2) and proposition (4.2). First, in the event that resident strains are purely lytic ($p = 0$), then, we have remark (6).

Remark 6 *We assume the resident viral strain is the purely lytic strategy ($p = 0$).*

(i) If the virus-free equilibrium of model [1.1] satisfies $\mathcal{R}^{hor}(S^*) < \mathcal{R}^{ver}(S^*)$, where $\mathcal{R}^{hor}(S^*)$ and $\mathcal{R}^{ver}(S^*)$ are given by Eq. [2.7], the viral strains with more lysogenic strategies (i.e., $0 < p_m \leq 1$) can invade the stable resident endemic equilibrium.

(ii) If the virus-free equilibrium of model [1.1] satisfies $\mathcal{R}^{hor}(S^*) > \mathcal{R}^{ver}(S^*)$, where $\mathcal{R}^{hor}(S^*)$ and $\mathcal{R}^{ver}(S^*)$ are given by Eq. [2.7], the viral strains with more lysogenic strategies (i.e., $0 < p_m \leq 1$) can invade the stable resident endemic equilibrium if $\mathcal{R}_+^{hor} < \mathcal{R}_+^{ver}$, where $\mathcal{R}_+^{hor}$ and $\mathcal{R}_+^{ver}$ are given by Eq. [4.3]. In contrast, the viral strains with more lysogenic strategies cannot invade the stable resident endemic equilibrium if $\mathcal{R}_+^{hor} > \mathcal{R}_+^{ver}$.

(iii) If the virus-free equilibrium of model [1.3] satisfies $\mathcal{R}^{hor}(S^*) < \mathcal{R}^{ver}(R^*)$, where $\mathcal{R}^{hor}(S^*)$ and $\mathcal{R}^{ver}(R^*)$ are given by Eq. [2.13], the viral strains with more lysogenic strategies (i.e., $0 < p_m \leq 1$) can invade the stable resident endemic equilibrium.

(iv) If the virus-free equilibrium of model [1.3] satisfies $\mathcal{R}^{hor}(S^*) > \mathcal{R}^{ver}(R^*)$, where $\mathcal{R}^{hor}(S^*)$ and $\mathcal{R}^{ver}(R^*)$ are given by Eq. [2.13], the viral strains with more lysogenic strategies (i.e., $0 < p_m \leq 1$) can invade the stable resident endemic equilibrium if $\mathcal{R}_+^{hor} < \mathcal{R}_+^{ver}$, where $\mathcal{R}_+^{hor}$ and $\mathcal{R}_+^{ver}$ are given by Eq. [4.7]. In contrast, the viral strains with more lysogenic strategies cannot invade the stable resident endemic equilibrium if $\mathcal{R}_+^{hor} > \mathcal{R}_+^{ver}$.

Second, in the event that the resident strain is purely lysogenic ($p = 1, \gamma = \gamma_{min}$) and the susceptible cell population is positive at the resident equilibrium, $S^+ > 0$, then we arrive at remark (7). Note that the invasion scenario of $S^+ = 0$ is provided in remark (5).

Remark 7 *We assume the resident viral strain is the purely lysogenic strategy ($p = 1, \gamma = \gamma_{min}$) and the susceptible cell population is positive at the resident equilibrium, $S^+ > 0$.*

(i) If the virus-free equilibrium of model [1.1] satisfies $\mathcal{R}^{hor}(S^*) < \mathcal{R}^{ver}(S^*)$, where $\mathcal{R}^{hor}(S^*)$ and $\mathcal{R}^{ver}(S^*)$ are given by Eq. [2.7], the viral strains with more lytic strategies (i.e., $0 \leq p_m < 1$ and $\gamma_{min} < \gamma_m \leq \gamma_{max}$) cannot invade the stable resident endemic equilibrium.

(ii) If the virus-free equilibrium of model [1.1] satisfies $\mathcal{R}^{hor}(S^*) > \mathcal{R}^{ver}(S^*)$, where $\mathcal{R}^{hor}(S^*)$ and $\mathcal{R}^{ver}(S^*)$ are given by Eq. [2.7], the viral strains with more lytic strategies (i.e., $0 \leq p_m < 1$ and $\gamma_{min} < \gamma_m \leq \gamma_{max}$) can invade the stable resident endemic equilibrium if $\mathcal{R}_+^{hor} > \mathcal{R}_+^{ver}$, where $\mathcal{R}_+^{hor}$ and $\mathcal{R}_+^{ver}$ are given by Eq. [4.3]. In contrast, the viral strains with more lytic strategies cannot invade the stable resident endemic equilibrium if $\mathcal{R}_+^{hor} < \mathcal{R}_+^{ver}$.

(iii) If the virus-free equilibrium of model [1.3] satisfies $\mathcal{R}^{hor}(S^*) < \mathcal{R}^{ver}(R^*)$, where $\mathcal{R}^{hor}(S^*)$ and $\mathcal{R}^{ver}(R^*)$ are given by Eq. [2.13], the viral strains with more lytic strategies (i.e., $0 \leq p_m < 1$ and $\gamma_{min} < \gamma_m \leq \gamma_{max}$) cannot invade the stable resident endemic equilibrium.

(iv) If the virus-free equilibrium of model [1.3] satisfies $\mathcal{R}^{hor}(S^*) > \mathcal{R}^{ver}(R^*)$, where $\mathcal{R}^{hor}(S^*)$ and $\mathcal{R}^{ver}(R^*)$ are given by Eq. [2.13], the viral strains with more lytic strategies (i.e., $0 \leq p_m < 1$ and $\gamma_{min} < \gamma_m \leq \gamma_{max}$) can invade the stable resident endemic equilibrium if $\mathcal{R}_+^{hor} > \mathcal{R}_+^{ver}$, where $\mathcal{R}_+^{hor}$ and $\mathcal{R}_+^{ver}$ are given by Eq. [4.7]. In contrast, the viral strains with more lytic strategies cannot invade the stable resident endemic equilibrium if $\mathcal{R}_+^{hor} < \mathcal{R}_+^{ver}$.

By theorem (1), the maximal strategies, i.e., the strategies that maximize $\mathcal{R}_0$, are either purely lytic strategy or the purely lysogenic strategy. For model [1.1] and model [1.3], when the resident strains are the maximal strategies, we provide remark (8).

Remark 8 *(i) If the purely lysogenic strategy maximizes $\mathcal{R}_0$, then no other strategy can invade the endemic equilibrium for the purely lysogenic strategy.*

(ii) If the purely lytic strategy maximizes $\mathcal{R}_0$, then no other strategy can invade the endemic equilibrium for the purely lytic strategy, provided $\mathcal{R}_+^{hor} > \mathcal{R}_+^{ver}$ holds. Otherwise, if $\mathcal{R}_+^{hor} < \mathcal{R}_+^{ver}$, the endemic equilibrium for the purely lytic strategy can be invaded by viral strains with more temperate strategies (i.e., $p_r < p_m \leq 1$ and $\gamma_{min} \leq \gamma_m < \gamma_r$).

C. Application to model variants with super-infection. In this section, we detail the invasion analysis for model variants of models [1.1] and [1.3] that include super-infection. we explore two cases: (i) super-infection occurs, but lysogens are not killed by obligately lytic viruses (i.e., super-infection immunity is present) and (ii) super-infection occurs, and lysogens are killed by obligately lytic viruses (i.e., super-infection immunity is not present).

(i) Super-infection immunity is present: Suppose the viruses can be absorbed into all the cells but only infect the susceptible cells, in other words, the infected cells are 'sinks'. To incorporate this, we replace the equation of $\dot{V}$ in model [1.1] and model [1.3] by

$$\dot{V} = \beta\eta I - \phi N V - mV, \qquad [4.12]$$

where $N = S + E + L + I$. First of all, we note that the interactions between viruses and infected cells are considered 'higher-order' terms at the virus-free equilibrium, Eq. [2.1] and Eq. [2.3], which will vanish under the linearizations of model [1.1] and model [1.3]. The viral invasion analysis at the virus-free equilibrium is the same as the case of no super-infection, and the maximal strategies are still either the purely lytic strategy or the purely lysogenic strategy. At the stable resident endemic equilibrium, the interactions between the mutant viral strains and the present infected cells (i.e., infected cells in the resident subsystem) are not 'higher-order' terms. We still use the NGM approach to study the mutants invasion. Here we need to replace $\mathcal{R}_+^{hor}$ in Eq. [4.3] and Eq. [4.7] by

$$\mathcal{R}_+^{hor} = \frac{\beta\eta\phi S^+\lambda}{(\eta + d_I)(\phi N^+ + m)(\lambda + d_E)} \qquad [4.13]$$

where $N^+ = S^+ + E^+ + L^+ + I^+$, and the other components in the next-generation matrices, Eq. [4.2] and Eq. [4.6] are unchanged but the resident equilibrium is obtained subject to the model [1.1] and model [1.3] with modified viral dynamics equation, Eq. [4.12]. Working through the same arguments in the SI Appendix - 4B, then remark (6), remark (7) and remark (8) still hold.

(ii) Super-infection immunity is not present : Here we assume all viruses infect all cell types, however in contrast to the prior analysis, we assume the purely lytic viruses ($p = 0$) can redirect the lysogens, L, to the exposed cells, E and eventually the infected cell type. Note that the interactions between viruses and infected cells are considered 'higher-order' terms at the virus-free equilibrium, Eq. [2.1] and Eq. [2.3], which will vanish under the linearizations of model [1.1] and model [1.3]. Hence, the viral invasion analysis at the virus-free equilibrium is the same as the case of no super-infection, and the maximal strategies are still either the purely lytic strategy or the purely lysogenic strategy.

First, consider the case where the purely lytic strategy ($p = 0$) is the resident viral strain. The mutant strains are the viral strains with more temperate strategies (i.e., $0 < p_m \leq 1$). The evolutionary invasion analysis is the same as when super-infection immunity is present.

Second, consider the case where the purely lysogenic strategy ($p = 1, \gamma = \gamma_{min}$) is the resident viral strain and the mutant strain is purely lytic ($p_m = 0$). Then, the linearized mutant-subsystem (i.e., linearized E_m, I_m, V_m-subsystem) is

$$\begin{aligned} \dot{E}_m &= \phi(S^+ + L^+)V_m - \lambda E_m - d_E E_m \\ \dot{I}_m &= \lambda E_m - \eta I_m - d_I I_m \\ \dot{V}_m &= \beta\eta I_m - \phi N^+ V_m - mV_m \end{aligned} \qquad [4.14]$$

where S^+, L^+ are the susceptible cells population density and lysogens population density at the resident equilibrium, and $N^+ = S^+ + E^+ + L^+ + I^+$ is the total cells population density. By the NGM approach, the invasion fitness of the mutant strain with purely lytic strategy is

$$\widetilde{\mathcal{R}_+^{hor}} = \frac{\beta\eta\phi(S^+ + L^+)\lambda}{(\eta + d_I)(\phi N^+ + m)(\lambda + d_E)}. \qquad [4.15]$$

Since lysogens are susceptible to the purely lytic viruses, the relevant results in remark (6), remark (7) and remark (8) no longer hold. Instead, the purely lytic viruses can invade the resident equilibrium established by the purely lysogenic strategy if $\widetilde{\mathcal{R}_+^{hor}} > 1$.

5. Model Parameters

Here we present the parameters used to support the figures presented in this study.

Table S1. Parameters of model (1.1), source from (6, 7)

Parameters	Value	Unit
r_L, maximal cellular growth rate of lysogens	1.2	h^{-1}
r_S, maximal cellular growth rate of susceptible cells	$0.2 + 10^{-4} \sim 20$	h^{-1}
d_E, cellular death rate of exposed infected cells	0.2	h^{-1}
d_L, cellular death rate of lysogens	0.2	h^{-1}
d_I, cellular death rate of lytic infected cells	0.2	h^{-1}
K, carrying capacity	2×10^8	ml^{-1}
λ, transition rate from exposed state to fated determined states	2	h^{-1}
η, lysis rate	1	h^{-1}
β, burst size	50	
ϕ, adsorption rate	3.4×10^{-10}	ml/h
m, virion decay rate	0.4	h^{-1}

Table S2. Parameters of model (1.2), source from (1)

Parameters	Value	Unit
r_L, growth rate of infected cells	1.4	h^{-1}
r_S, growth rate of susceptible cells	$0.75 + 10^{-4} \sim 36.5$	h^{-1}
K, carrying capacity of bacteria	10^9	cells/ml
δ, fidelity of vertical transmission	1	
β, burst size	200	phage/cell
m, dilution rate	0.75	h^{-1}
b, probability of fusion after adsorption	10^{-2}	
ϕ, adsorption constant	10^{-8}	$h^{-1}cell^{-1}$

Table S3. Parameters of model (1.3), source from (2, 7)

Parameters	Value	Unit
e, conversion efficiency	5×10^{-7}	μg
d_R, decay rate of resources	0.2	h^{-1}
μ_{max}, maximum growth rate of cells	1.2	h^{-1}
R_{in}, half-saturation constant	4.0	μg/ml
d_E, cellular death rate of exposed infected cells	0.2	h^{-1}
d_L, cellular death rate of lysogens	0.2	h^{-1}
d_I, cellular death rate of lytic infected cells	0.2	h^{-1}
λ, transition rate from exposed state to fated determined states	2	h^{-1}
η, lysis rate	1	h^{-1}
β, burst size	50	
ϕ, adsorption rate	3.4×10^{-10}	ml/h
m, virion decay rate	0.4	h^{-1}
α_S, selection coefficient	$-1 \sim 0.4$	
J, influx rate of resources	$0.5 \sim 17$	(μg/ ml) h^{-1}

Table S4. Parameters of model (1.4), source from (2)

Parameters	Value	Unit
e, conversion efficiency	5×10^{-7}	$\mu g/$ cell
ρ, flow rate	0.2	h^{-1}
b, maximum growth rate of cells	0.7	h^{-1}
R_{in}, half-saturation constant	4.0	μg/ml
ν, prophage loss rate by vegetative segregation	10^{-3}	(1/cell) h^{-1}
β, burst size	100	phage/cell
ϕ, phage adsorption rate	10^{-9}	(ml/phage) h^{-1}
α_S, selection coefficient	$-1 \sim 0.3$	
C, resource concentration in the reservoir	$0.6 \sim 52$	$\mu g/$ ml

References

1. TW Berngruber, R Froissart, M Choisy, S Gandon, Evolution of virulence in emerging epidemics. *PLOS Pathog.* **9**, 1–8 (2013).
2. FM Stewart, BR Levin, The population biology of bacterial viruses: Why be temperate. *Theor. Popul. Biol.* **26**, 93 – 117 (1984).
3. O Diekmann, JAP Heesterbeek, MG Roberts, The construction of next-generation matrices for compartmental epidemic models. *J. The Royal Soc. Interface* **7**, 873–885 (2010).
4. R Levins, Discussion paper: the qualitative analysis of partially specified systems. *Annals New York Acad. Sci.* **231**, 123–138 (1974).
5. A Hurford, D Cownden, T Day, Next-generation tools for evolutionary invasion analyses. *J. The Royal Soc. Interface* **7**, 561–571 (2010).
6. JS Weitz, *Quantitative viral ecology: dynamics of viruses and their microbial hosts.* (Princeton University Press) Vol. 73, (2015).
7. JS Weitz, G Li, H Gulbudak, MH Cortez, RJ Whitaker, Viral invasion fitness across a continuum from lysis to latency. *Virus Evol.* **5**, vez006 (2019).